

Insights into the mechanobiology of cancer metastasis via microfluidic technologies

Cite as: APL Bioeng. 8, 021506 (2024); doi: 10.1063/5.0195389

Submitted: 2 January 2024 · Accepted: 20 May 2024 ·

Published Online: 3 June 2024



View Online



Export Citation



CrossMark

Lanfeng Liang,¹  Xiao Song,²  Hao Zhao,^{2,3}  and Chwee Teck Lim^{1,2,4,a)} 

AFFILIATIONS

¹Mechanobiology Institute, National University of Singapore, Singapore

²Department of Biomedical Engineering, National University of Singapore, Singapore

³Integrative Sciences and Engineering Programme, NUS Graduate School, National University of Singapore, Singapore

⁴Institute for Health Innovation and Technology (iHealthtech), National University of Singapore, Singapore

Note: This paper is part of the special issue on Physical Sciences Approaches to Cancer Research.

a) Author to whom correspondence should be addressed: ctlm@nus.edu.sg

ABSTRACT

During cancer metastasis, cancer cells will encounter various microenvironments with diverse physical characteristics. Changes in these physical characteristics such as tension, stiffness, viscosity, compression, and fluid shear can generate biomechanical cues that affect cancer cells, dynamically influencing numerous pathophysiological mechanisms. For example, a dense extracellular matrix drives cancer cells to reorganize their cytoskeleton structures, facilitating confined migration, while this dense and restricted space also acts as a physical barrier that potentially results in nuclear rupture. Identifying these pathophysiological processes and understanding their underlying mechanobiological mechanisms can aid in the development of more effective therapeutics targeted to cancer metastasis. In this review, we outline the advances of engineering microfluidic devices *in vitro* and their role in replicating tumor microenvironment to mimic *in vivo* settings. We highlight the potential cellular mechanisms that mediate their ability to adapt to different microenvironments. Meanwhile, we also discuss some important mechanical cues that still remain challenging to replicate in current microfluidic devices in future direction. While much remains to be explored about cancer mechanobiology, we believe the developments of microfluidic devices will reveal how these physical cues impact the behaviors of cancer cells. It will be crucial in the understanding of cancer metastasis, and potentially contributing to better drug development and cancer therapy.

© 2024 Author(s). All article content, except where otherwise noted, is licensed under a Creative Commons Attribution-NonCommercial 4.0 International (CC BY-NC) license (<https://creativecommons.org/licenses/by-nc/4.0/>). <https://doi.org/10.1063/5.0195389>

I. INTRODUCTION

Metastasis remains a major clinical challenge in most cancer types and continues to be a poorly understood aspect of cancer pathogenesis.¹ Such understanding of what is cancer metastasis is essential for us to effectively combat cancer. To do so, we must first delve into the progression of each step in the metastatic cascade and understand what is crucial in the development of metastatic disease.

The progression of metastatic disease is a multifaceted and intricate process, typically encompassing a series of sequential stages: cancer cells invade the surrounding tissue (invasion), then enter the lymphatic and/or blood circulatory system (intravasation), travel through and survive the bloodstream (circulating), escape from the blood vessel (extravasation), and finally adapt and grow in a colonial environment (metastatic colony).^{2,3} Metastasis is a dynamic process

involving cancer cells have to travel through and interact with native tissues or organ microenvironments. One vital aspect of these diverse microenvironments is their physical properties, which could significantly influence the outcome of metastasis. For example, increased extracellular fluid viscosity can enhance cancer dissemination;⁴ the confined tissue or ECM space can deform the metastasizing cancer cells, leading to DNA damage and even cell death;⁵ high blood fluid shear stresses can destroy both navigating and arresting circulating tumor cells (CTCs).^{6,7} As such, these mechanical environments directly exert physical forces on cancer cells. Nevertheless, our understanding of these interactions between the physical microenvironment and metastasizing cancer cells, and how these physical microenvironments drive the metastasis process, remains considerably limited. A comprehensive understanding of the mechanobiological mechanisms

might provide more precise and potential targets to combat cancer metastasis.

In clinical practice, there is an assumption that mutated genes or mis-expressed proteins in cancer cells are responsible for driving the occurrence of lethal metastasis.⁸ However, we lack understanding of what these genes and proteins are and how they function. One of the primary barriers to unraveling these mechanisms is the lack of a suitable model. While studying cancer metastasis in animal models has been considered a valuable approach, observing these interactions with the physical microenvironment at the cellular scale within *in vivo* models is exceptionally challenging or almost impossible. Currently, most *in vivo* studies only allow tracking the metastatic outcomes, resembling a black box experiment.⁹ Even, the simplest intravital tracking requires complex and costly imaging facilities, which hinders our ability to fully comprehend the intricacies of metastasis. Consequently, there is a significant motivation to find a straightforward but physiologically relevant model that enables the investigation of the molecular mechanisms underlying each step of metastasis.

An interdisciplinary approach involving biology and engineering science provides a promising opportunity. With an increasing understanding of the *in vivo* physical microenvironment, more researchers are utilizing an engineering strategy, especially microfluidics, to replicate such microenvironments found *in vivo*. This approach simplifies and re-establishes mechanical microenvironment on *in vitro* devices, enabling discoveries at the cellular and even molecular scale. Therefore, our goal is to review the biomimetic engineering microfluidics developed in current years to mimic the physiologically physical microenvironment during cancer metastasis, along with their applications in cancer research. In this review, we will cover the metastatic cascade, first introducing the physical characteristics of each metastatic microenvironment and the tools used to measure these properties. Subsequently, we will focus on the *in vitro* microfluidic devices that have been developed to mimic *in vivo* physical microenvironments. We will also delve into the study of mechanobiological mechanisms based on these *in vitro* devices. Finally, we will discuss the potential of clinical applications targeting the biophysical features, with the ultimate aim of advancing anti-cancer metastasis treatments.

II. PHYSICAL TRAITS INFLUENCING CANCER METASTASIS

Mechanical forces play a critical role in the functions and behaviors of cells, tissues, and organs, especially in the context of cancer metastasis. During the metastatic process, cancer cells encounter and respond to various mechanical stimuli from their environments. These cancer cells can convert mechanical signals into biochemical responses, influencing key biological processes such as survival, proliferation, and dissemination.¹⁰ Additionally, cancer cells can process these mechanical signals through mechanotransduction, where epigenetic remodeling enhances tumor cell extravasation and other functions related to metastasis.^{11,12} While the use of microfluidics has revealed numerous biological insights about the interaction between cancer cells and their surrounding environments, many physical aspects remain unexplored due to the absence of appropriate models. Understanding the types of physical cues along the metastatic cascade is crucial before reconstructing appropriate microfluidic models and exploring biological questions.

A. Matrix stiffness

Matrix stiffness is one of the most widely studied physical properties, particularly in the context of cancer study [Fig. 1(b)]. The concept refers to the mechanical property of the extracellular matrix (ECM) and tissue that describes their resistance to deformation or rigidity in response to an applied force.

In cancer metastasis, cancer cells must interact with various ECM or tissue environments with different stiffness properties. Since many studies show there is a clear distinction in the mechanical properties between healthy ECM and pathological ECM, quantification of ECM stiffness is of particular interest in cancer research. Using atomic force microscope (AFM), which can apply a controlled force to the ECM and measure the resulting deformations, healthy ECM tissues (0.4–2.5 kPa) were found to be softer when compared to malignant tissues (2.5–5 kPa) in breasts.^{13,14} This stiffening of malignant tissues has been found in various cancer types, including pancreas (healthy tissues: 0.5–1 kPa vs malignant tissues: 0.75–2 kPa),¹⁵ lung (healthy tissues: 1.61–5.83 kPa vs malignant tissues: 17.68–43.31 kPa),¹⁶ liver (healthy tissues: 3.9–10 kPa vs malignant tissues: 7.8–60 kPa),¹⁷ and glioma (healthy tissues: 0.05–250 Pa vs malignant tissues: 50–1500 Pa).¹⁸ Understanding the role of matrix stiffness will offer deeper insights into its biological impact on cancer development and metastasis.

B. Matrix viscoelasticity

In the human body, cells, tissues and ECM exhibit viscoelastic properties. While viscoelasticity and stiffness are correlative mechanical parameters, they fundamentally represent different aspects of a material's physical properties. Viscoelasticity refers to the time-dependent response to return to its original shape after the removal of an applied force and encompasses both viscous and elastic characteristics.¹⁹ Stiffness, on the other hand, measures a resistance to deformation when a force is applied.²⁰

Similar to matrix stiffness, interaction with varying matrix viscoelasticity occurs throughout the metastatic progression. However, our understanding of this interaction and its underlying biological impact remains limited. Characterization of viscoelastic behavior in metastatic matrix is high priority, and experiments are typically conducted using a step-hold approach. Currently, AFM has emerged as a prevalent microrheology tool for characterizing both elastic and viscoelastic properties of biological samples.²¹ By adding a hold phase in each force curve measurement, AFM enables the determination of elastic properties with a high-resolution distribution map. Despite ongoing efforts to quantify viscoelastic parameters in some biological structures,^{22–24} a standardized method of quantification does not yet exist. Particularly, this challenge is compounded by the fact that most biological structures do not follow linear elastic behavior, indicating that the derived viscoelastic parameters should not be influenced by the applied force or indentation depth.²¹ Beyond the complexities of characterizing viscoelastic properties, the development of viscoelastic materials with biocompatibility presents another challenge in understanding how viscoelasticity affects cancer metastasis.²²

C. Tumor solid stress

Solid stress becomes pronounced within the solid tumor microenvironment and emerges as a crucial marker during tumor

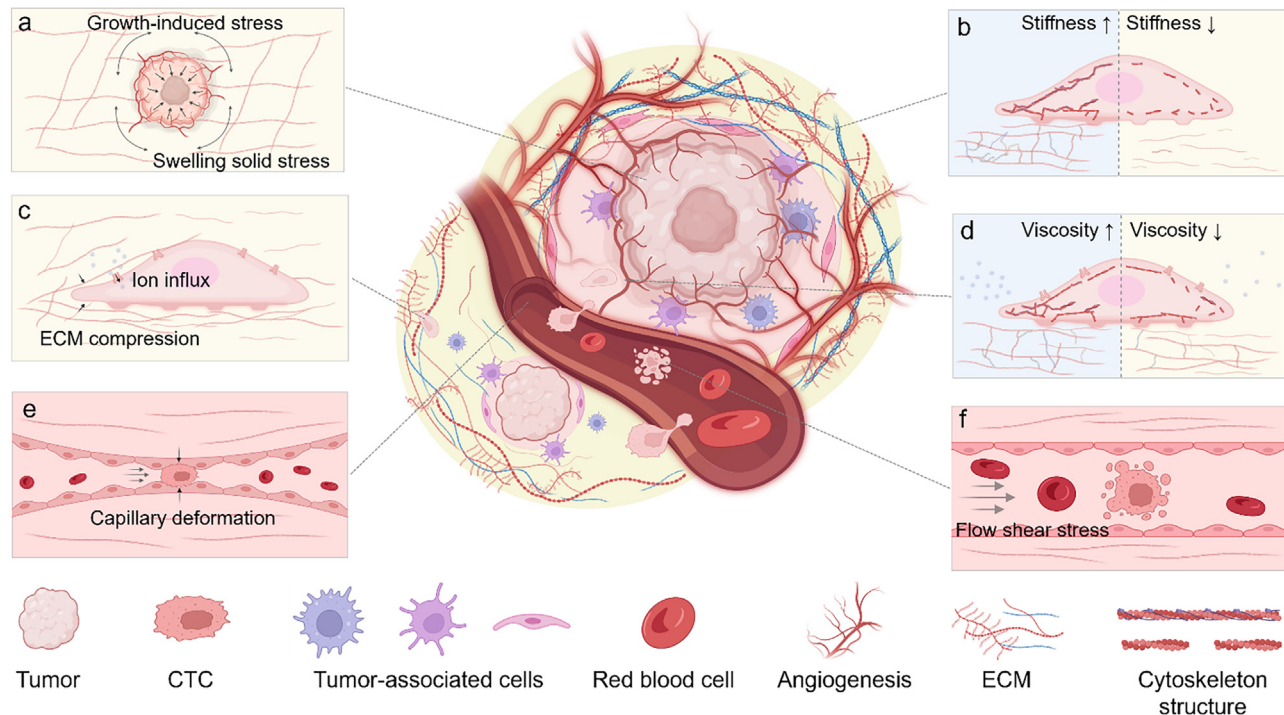


FIG. 1. Engineering the physical microenvironments during cancer metastasis. (a) As tumor grows, tumor cells have to undergo higher growth-induced mechanical stress and swelling solid stress due to interactions with neighboring tissue cells and ECM network. (b) Higher stiffness environment facilitates cell growth, survival, and migration. (c) Invasion typically requires cancer cells to squeeze through the ECM network, where dense ECM network will deform cell body and activate some ion channels. (d) Increasing extracellular viscosity promotes an ARP2/3-mediated dense actin network at the leading edge, enhancing cell migration. (e) Navigating in capillary channels with narrow diameter can deform cytoskeleton and even nucleus, which potentially influence the epigenetics of cancer cells. (f) High fluid shear stress can induce apoptosis of circulating tumor cells (CTCs).

progression.²⁵ In solid tumor, the stiffness is due to the accumulation of ECM, while the physical forces exerted by their non-fluid component during tumor growth contributes to solid stress.²⁶ In a study, tumors embedded in 2% agarose was cut, allowing the release of the solid stress in the planar cut direction.²⁷ Subsequently, the solid stress induced deformation was measured using high-resolution ultrasound probe and solid stress was calculated using Hooke's Law. Using this 2D mapping approach, it was found that the maximum value of the solid stress ranged from 0.21 kPa (1.56 mm Hg) in brain tumor to 7 kPa (52.5 mm Hg) in highly desmoplastic pancreatic tumors.²⁸

Solid stress, mechanical forces exerted by non-fluid component within tumor, can be broadly categorized into three types, including tumor growth-induced stress, swelling stress and externally applied stress [Fig. 1(a)].²⁹ Uncontrolled cancer cell proliferation and expansion contribute to the grow-induced stress, exerting tensile stress on the collagen fibers in tumor microenvironment while the compressive stress arises from the resistance to the cancer cell expansion by hyaluronan in tumor microenvironment.³⁰ Swelling solid stress results from the interaction between collagen and hyaluronan within the tumor microenvironment.³¹ Hyaluronan, with negative charges, attracts significant amounts of the interstitial fluid and causes electrostatic repulsion, driving a swelling effect.³² Consequently, tensile stress emerges from the stretching and stiffening of collagen fibers by the elevated

swelling. Collectively, the growth-induced swelling stress contributes to the main solid stress within the tumors.³³ In fact, it is revealed that within the tumor, the solid stress is compressive in all the directions, whereas at the boundary, the stresses are tensile in the circumferential direction and compressive in the radial direction, respectively.²⁷ Externally applied stress generated by the host tissue to counteract tumor expansion exerts compressive stress on the tumor at the tissue level.³⁴

D. Environmental confinement

The physical confinement is a key mediator of metastasis and is involved in the process of invasion, intravasation, bloodstream circulation and extravasation.^{9,35} Cancer cells, escaping from the primary tumors and invading into and through the dense ECM, will penetrate through constriction pores with diameters varying from less than 1 to 20 μm , and with channel-like and fiber-like tracks ranging from 3 to 30 μm in width and from 100 to 600 μm in length [Fig. 1(c)].⁵ Matrix degradation is required when the cross-sectional area of the pores is smaller than $8\mu\text{m}^2$ with the help of matrix metalloproteinases (MMPs).³⁶ After squeezing through the tight junction between endothelial cells of less than 1 μm in width, intravasating cancer cells enter the blood vessels and circulate through the bloodstream, known as CTCs.³⁷ CTCs get arrested when encountering the capillary beds, with

the capillary diameters going down to $3\ \mu\text{m}$ [Fig. 1(e)]. Consequently, only a small proportion of CTCs will successfully undergo extravasation and form distal colonies.³⁸ During transition from these micrometer-sized pores and constrictions, extensive cell and nucleus deformation occur, resulting in approximately 90% cell death as well as more invasive phenotype.³⁹

E. Flow shear stress

One crucial biomechanical force in cancer metastasis is fluid shear stress (FSS), induced by the frictional forces of blood fluids.² The value of FSS is directly related to fluid velocity, which exhibits high heterogeneity in the circulatory system [Fig. 1(f)]. By observing the movement of erythrocytes, the most common type of blood resident cells, researchers could visualize blood flows and measure their mean flow velocity in various organs.^{40,41} Experimentally measured values of blood flow velocities in the cerebral capillaries suggest variations mainly from $0.79 \pm 0.03\ \text{mm/s}$, faster than velocities of $0.05\text{--}0.2\ \text{mm/s}$, observed in the liver. In addition, the developments of laser-based and ultrasound Doppler flowmetry, which are based on the Doppler effect, increase efficiency for the detection and visualization of capillary blood flow ($0.3\text{--}1.7\ \text{mm/s}$), which is currently commercialized as a noninvasive detection method in clinical medicine.^{42,43} By using computational modeling, the environmental blood flow in which CTCs are exposed in the microcirculation produces cell surface fluid shear stress of $2\text{--}40\ \text{dyn/cm}^2$.^{44,45}

F. Extracellular fluid viscosity

The extracellular fluid (ECF) contains plasma proteins and various solutes that are filtered from the circulating system.⁴⁶ Cells *in vivo* always reside in fluids with viscosities that are significantly higher than those of cell culture media, potentially due to the dissolution of some extracellular macromolecules such as hyaluronic acids and soluble collagen in physiological environment.⁴⁷

Typically, the viscosity of ECF in normal tissue is about 0.77 centipoise (cp), while viscosity of ECF in some pathological lesions can increase by up to three orders of magnitude.⁴⁸ Within the tumor microenvironment, the presence of macromolecules such as mucins, soluble collagen, and hyaluronic acids—secreted by both epithelial cells of host tissues and tumor cells—further elevates ECF viscosity.⁴⁹ This increase in macromolecules is often compounded by leakage from blood and lymphatic vessels during tumor growth. The primary tumor site experiences an augmentation in macromolecular crowding due to the breakdown of the extracellular matrix, for instance, by MMPs during invasion, leading to a further increase in ECF viscosity.⁵⁰ Currently, it is demonstrated that this biophysical property affects modes of cancer cell migration [Fig. 1(d)].⁴

To sum up, study of physical properties of the various components to better understand their influence on cancer cell metastasis will enable more precise *in vitro* reconstruction and study of cell behaviors as well as their underlying mechanisms within physiologically relevant environment. The advancement in current engineering tools will provide the needed physical information on cells and tissues in both their normal and malignant states. We have summarized the engineering approaches and the mechanical properties of biological entities involved in cancer metastasis in Table I.^{14,15,18,51–79}

III. ON-CHIP PRIMARY TUMOR AND TUMOR PHYSICAL ENVIRONMENT

The process of cancer metastasis initiates at the primary tumor site, where tumor cells divide uncontrollably and start to invade surrounding tissues, reach the circulatory system, and eventually form metastatic lesions. In the primary tumor, tumor cells exhibit a time-dependent response as they interact with various physical extracellular microenvironments. These biomechanical factors, including the stiffness of the ECM, fluid shear stress, as well as compressive and tensile forces induced by tumor growth (Fig. 2),^{80–83} play a regulatory role in tumor cell proliferation and subsequent dissemination.

A. Effects of ECM stiffness on tumor development

The ECM, a complex network of hydrated macromolecular proteins and sugars, undergoes dynamic changes during tumor progression. The increased stiffness of the ECM microenvironment prompts tumor cells to reorganize their cytoskeleton structure and elevate cellular tension through Rho/ROCK signaling activation.⁸⁴ Moreover, cells also have the ability to sense their surrounding stiffness. As one of the molecular signal factors for mechanotransduction, yes-associated protein (YAP) serves as a transcriptional coactivator. Its function is associated with nucleus translocation, which is triggered by mechanical forces.^{85–87} A relatively higher stiffness microenvironment exerts a force to open cellular nuclear pores, translocating YAP/TAZ into the nucleus, thus activating the cell proliferation-associated pathways. In some cases, the activation of YAP in a higher stiffness microenvironment enhances migration on non-metastatic primary tumor cells, promoting the spread of cancerous cells from the primary tumor.⁸⁸ In addition, transient receptor potential vanilloid 4 (TRPV4) can act as a sensor to sense surrounding ECM stiffness in tumor cells. Increasing matrix stiffness promotes calcium influx, resulting in matrix stiffness-induced epithelial-mesenchymal transition by enhancing Akt function and downregulating E-cadherin.⁸⁹

B. Effects of fluid shear stress on primary tumor

In tumor lesions, fluid shear stress, generated by the movement of interstitial fluid, blood, or lymph fluid, is a highly hemodynamic force controlled by the movement of blood through the circulatory system. As tumor growth progresses, the increasing need for nutrients and oxygen supply drives the tumor to release signaling molecules, such as vascular endothelial growth factor (VEGF), for stimulating more blood vessels and altering fluid volume in the surrounding tissues. Compared with a static environment, current, microfluidic-based studies suggest that low fluid shear stress enhances cancer migration.^{44,90} Contacting with a low FSS ($\sim 0.1\ \text{dyn/cm}^2$) environment activates YAP and a ROCK-LIMK-cofilin axis, enhancing the formation of filopodia. In addition, these new blood vessels, known as angiogenesis or lymph-angiogenesis, not only serve as a nutrient duct but also provide pathways for cancer dissemination.^{91,92} Unfortunately, most studies targeting the influence of FSS are based on a mono-layer model rather than a 3D spherical tumor model.⁸⁰ Although current organoid technology involves cellular heterogeneity to mimic *in vivo* tumors, engineering a 3D tumor model with vasculature in microfluidic devices is still at its early stage.^{93,94} We believe that advancements in engineering methods will make it possible to replicate this “tumor angiogenesis

TABLE I. Engineering approaches in measuring the physical properties of biological entities involved in metastasis.

Organ	Cell/tissue	Experimental setting	Methods	Physical properties	Measuring parameters	References
Bladder	Cell	<i>In vitro</i>	AFM	Young's modulus (E)	RT112 (Normal): E = 1738 ± 54 Pa (nucleus area); T24 (Malignant): E = 1182 ± 154 Pa	51
	Cell	<i>In vitro</i>	AFM	Young's modulus (E)	HCV29 (Normal): E = 3.09 ± 0.78 kPa; T24 (Malignant): E = 0.78 ± 0.2 kPa	52
	Tissue, spheroid- liked organoids	<i>In vitro</i>	AFM	Young's modulus (E)	HCV29 spheroid (normal): E = 14.5 ± 2.2 kPa; T24 spheroid (Malignant): E = 2.7 ± 0.3 kPa	53
	Tissue	<i>In vitro</i>	Nanoindenter	Young's modulus (E)	Healthy bladder tissue (normal): E ~ 33 kPa; High-grade MICB tissue (Malignant): E ~ 2 kPa	54
Brain	Tissue, human tumor grows in mouse	<i>Ex vivo</i>	AFM	Young's modulus (E)	Normal brain: E ~ 0.4 kPa; GBM U87: E ~ 0.15 kPa; GBM MGG8: E ~ 0.1 kPa; BC BT474: E ~ 0.1 kPa)	55
	Tissue, mice brain section	<i>Ex vivo</i>	AFM	Young's modulus (E)	Uninjured contralateral corpus cal- losum: E = 12.01 ± 6.16; demyelin- ation (post 7 days of injection) E = 4.34 ± 2.55	56
	Tissue	<i>Ex vivo</i>	Objective shear wave elastography (SWE)	Young's modulus (E)	Normal brain tissue: E = 7.3 ± 2.1 kPa (n = 63); meningiomas: E = 33.1 ± 5.9 kPa (n = 16); low-grade gliomas: E = 23.7 ± 4.9 kPa (n = 14); high-grade gliomas: E = 11.4 ± 3.6 kPa (n = 18); metastasis: E = 16.7 ± 2.5 kPa (n = 15)	57
	Tissue	<i>In vivo</i>	Intravital micro- filming image	Blood flow velocity (ν)	Cerebral capillaries (2–5 μ m in diameter): ν = 0.73 ± 0.03 mm/s (n = 100)	40
Breast	Cell	<i>in vitro</i>	AFM	Young's modulus (E)	MCF10A: E = 341.91 ± 97.98 Pa; MCF7:	58

TABLE I. (Continued.)

Organ	Cell/tissue	Experimental setting	Methods	Physical properties	Measuring parameters	References
	Cell	<i>Ex vivo</i>	AFM	Young's modulus (E)	E = 285.13 ± 127.03 Pa; MDA-MB-231: E = 277.32 ± 63.13 Pa Normal breast cells: E = 1.93 ± 0.5 kPa; malignant breast cells: E = 0.5 ± 0.08 kPa	59
	Cell, patient-derived cells	<i>Ex vivo</i>	AFM	Young's modulus (E)	Normal breast cells: E = 1.7 ± 0.95 kPa; metastatic breast cancer cells: E = 0.2 ± 0.1 kPa	60
	Cell	<i>In vitro</i>	Optical tweezer microscopy	Young's modulus (E)	HBL-100: E = 23.5 ± 10.6 kPa; MCF7: E = 30.2 ± 15 kPa; MDA-MB-231: E = 12.6 ± 6.1 kPa	61
	Cell	<i>In vitro</i>	Microfluidic assay	Deformability (passing time)	MCF10A: ~2.2 s; MCF7: ~1.5 s	62
	Cell	<i>In vitro</i>	Traction force microscopy	Traction force (τ)	MCF10A: τ ~ 6 nN; MCF7: τ ~ 14 nN	63
	Tissue	<i>Ex vivo</i>	AFM	Young's modulus (E)	Normal breast tissue: E = 1.16 ± 0.2 kPa; malignant breast tissue: E = 1.54 ± 0.17 kPa	64
	Tissue	<i>Ex vivo</i>	AFM	Young's modulus (E)	Normal breast tissue: E ~ 0.4 kPa; malignant breast tissue: E ~ 1.2 kPa	18
	Tissue, spheroid-liked organoids	<i>In vitro</i>	Brillouin microscopy	Young's modulus (E)	Normal spheroid: E ~ 1.25 kPa (day 5); malignant breast tissue: E ~ 1 kPa (day 5)	65
	Tissue	<i>In vivo</i>	High-resolution ultrasonography	Solid stress (Ω)	Breast tumor: Ω ~ 0.05 kPa	55
Cervix	Cell	<i>In vitro</i>	AFM	Young's modulus (E)	END1: E = 5.5 ± 0.54 kPa; HeLa: E = 2.48 ± 0.5 kPa	66
	Cell	<i>In vitro</i>	AFM	Young's modulus (E)	Normal cervical epithelial cells (CRL2614): E = 1.20–1.32 kPa;	67

TABLE I. (Continued.)

Organ	Cell/tissue	Experimental setting	Methods	Physical properties	Measuring parameters	References
	Cell, patient-derived	<i>Ex vivo</i>	AFM	Young's modulus (E)	human cervical squamous carcinoma cells (CaSki): E = 0.35–0.47 kPa Normal cells: E = 2.05 ± 0.48 kPa; cancer cells: E = 2.8 ± 1.7 kPa	68
Colorectal	Tissue, patient-derived sample	<i>Ex vivo</i>	AFM	Young's modulus (E)	Normal tissue: E ~ 0.07 kPa; tumor epithelium: E ~ 0.15 kPa; tumor stroma: E ~ 0.2 kPa	69
	Tissue, patient-derived sample	<i>Ex vivo</i>	AFM	Young's modulus (E)	Primary tissue: E ~ 0.5 kPa; liver metastasis: E ~ 1.5 kPa	79
Kidney	Cell	<i>In vitro</i>	AFM	Young's modulus (E)	Non-tumorigenic cell line (RC124): E = 9.38 kPa; adenocarcinoma (ACHN): E = 2.48 kPa; carcinoma (A498): E = 7.41 kPa	23
	Tissue, rat	<i>In vivo</i>	Ultrasound	Blood flow speed (ν)	Normal kidney artery: ν = ~30 mm/s; Ischemic-reperfused kidney artery: ν < 10 mm/s	70
	Tissue, rat	<i>Ex vivo</i>	Water exchange	Molar solution of sodium chloride	Isotonicity: 0.20–0.27 within 90 mins	71
Liver	Cell	<i>In vitro</i>	Micropipette aspiration	Elastic coefficients (K) and viscous coefficient (μ)	Hepatocytes: K1 = 87.5 ± 12.1 N m ⁻² , K2 = 33.3 ± 10.3 N m ⁻² , μ = 5.9 ± 3.0 Pa s; hepatocellular carcinoma (HCC): K1 = 103.6 ± 12.6 N m ⁻² , K2 = 42.5 ± 10.4 N m ⁻² , μ = 4.5 ± 1.9 Pa s	24
	Tissue, patient-derived sample	<i>Ex vivo</i>	AFM	Young's modulus (E)	Neoplasm tissue: E = 0.42 ± 0.17 kPa;	72

TABLE I. (Continued.)

Organ	Cell/tissue	Experimental setting	Methods	Physical properties	Measuring parameters	References
	Tissue, patient-derived sample	<i>Ex vivo</i>	Ultrasound elastography	Young's modulus (E)	Paraneoplastic tissues: E = 1.10 ± 0.20 kPa Normal liver tissue: E = 3.6–4.1 kPa; Fibrotic liver tissues: E = 3.7–20 kPa; Hepatocellular carcinoma (HCC): E = 4.5–265 kPa	17
	Tissue	<i>In vitro</i>	Doppler ultrasound	Blood flow volume speed (ν)	Normal portal venous blood flow: $\nu = 864 \pm 188$ ml/min	73
	Tissue, mouse and rat	<i>In vivo</i>	<i>In situ</i> imaging	Blood flow speed (ν)	Zone 1 (mouse): $\nu = 1.39 \pm 0.78$ $\mu\text{m/s}$; Zone 3 (rat): $\nu = 1.25 \pm 0.09$ $\mu\text{m/s}$	41
	Tissue, rat	<i>Ex vivo</i>	Water exchange	Molar solution of sodium chloride	Isotonicity: 0.244–0.442 within 90 mins	71
Lung	Cell	<i>In vitro</i>	Micropipette aspiration	Young's modulus (E)	H23 cells: E = 0.46 ± 0.18 ; A549 cells: E = 1.39 ± 0.68	74
	Tissue	<i>Ex vivo</i>	AFM	Young's modulus (E)	Tumor-free lung tissue: E = 1.61 ± 3.97 kPa; tumor benign lung tissue: E = 17.68 ± 25.63 kPa	16
Melanoma	Cell, patient-derived cells	<i>Ex vivo</i>	AFM	Young's modulus (E)	WM115 (derived from primary tumor): E = 15 ± 8 kPa; WM266-4 (established from metastasis to the skin): E = 9 ± 4 kPa	75
Pancreas	Cell, patient-derived cells	<i>Ex vivo</i>	AFM	Young's modulus (E)	Normal pancreas: E = 2.7 ± 1.6 kPa; Metastatic PDAC: E = 0.6 ± 0.1 kPa	60
	Tissue	<i>In vitro</i>	AFM	Young's modulus (E)	Normal tissue: E ~ 500 Pa (overall); E ~ 1 kPa (upper quartile); PanIN: E ~ 750 Pa (overall); E ~ 2 kPa (upper quartile) PDAC:	15

TABLE I. (Continued.)

Organ	Cell/tissue	Experimental setting	Methods	Physical properties	Measuring parameters	References
	Tissue, rat	<i>Ex vivo</i>	Water exchange	Molar solution of sodium chloride	E ~ 1200 Pa (overall); E ~ 4 kPa (upper quartile) Isotonicity: 0.21 ~ 0.5+ within 90 mins	71
Prostate	Cell	<i>In vitro</i>	AFM	Young's modulus (E)	PZHPV-7: E = 3.09 ± 0.84 kPa; LNCaP: E = 0.45 ± 0.21 kPa; DU-145: E = 1.36 ± 0.42 kPa; PC-3: E = 1.95 ± 0.47 kPa	64
	Cell, cancer-associated fibroblasts	<i>Ex vivo</i>	Traction force microscopy	Traction force (τ)	Normal fibroblast: τ ~ 2 kPa; Cancer-associated fibroblast: τ ~ 3.5 kPa	76
Thyroid	Cell	<i>In vitro</i>	AFM	Young's modulus (E)	S748: E = 2211–6879 Pa, S277: E = 1189–1365 Pa	77
	Tissue, patient-derived tissue	<i>Ex vivo</i>	AFM	Young's modulus (E)	Papillary carcinomas: E = 1.7 ± 1.7 kPa; anaplastic carcinoma: E = 2.4 ± 2.2 kPa; poorly differentiated carcinomas: E = 0.78 ± 0.54 kPa	78

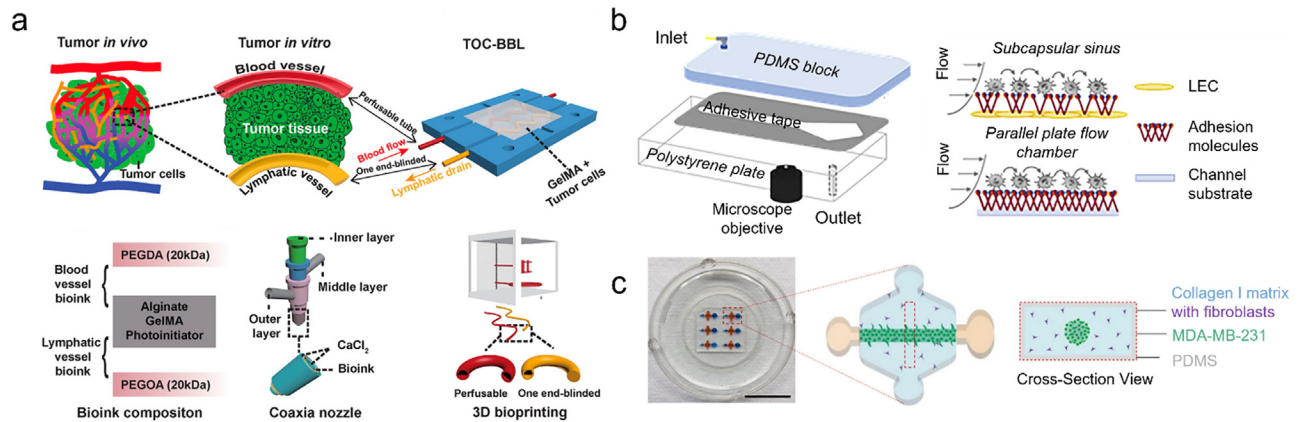


FIG. 2. *In vitro* strategies for studying the biomechanical properties of the primary tumor and the associated tumor ECM. (a) Sequential explanation of the tumor-on-a-chip with bio-printed blood and a lymphatic vessel pair (TOC-BBL) recapitulating the *in vivo* flow environment at the tumor site. Reproduced with permission from Cao *et al.*, *Adv. Funct. Mater.* **29**, 1807173 (2019). Copyright 2019 Authors, licensed under a Creative Commons Attribution (CC BY) international license.⁸⁰ (b) A lymph node subcapsular sinus micro-environment-on-a-chip system designed to study the effect of physiological shear flow in tumor microenvironment on lymphatic metastasis. Reproduced with permission from Birmingham *et al.*, *iScience* **23**, 101751 (2020). Copyright 2020 Authors, licensed under a Creative Commons Attribution (CC BY) 4.0 international license.⁸² (c) Schematic structure of a microfluidic model with 3D heterogeneous ECM components including fibroblast used for studying the effect of tumor ECM composition on breast cancer cell migration. Reproduced with permission from Lugo-Cintrón *et al.*, *Cancers* **12**, 1173 (2020). Copyright 2020 Authors, licensed under a Creative Commons Attribution (CC BY) license.⁸³

on-a-chip” model and provides more insights into how FSS regulates dissemination in primary tumor lesion.

C. Solid stresses within tumors

Tumor spheroids in a gel matrix are extensively employed to explore the effect of compressive stress.^{95,96} The expression of Bcl-2 was downregulated in response to the compressive stress, triggering caspase 3 nuclear translocation, and ultimately resulting in compression-induced cancer cell apoptosis.⁹⁵ Upregulated cell apoptosis events and defects in proliferation contribute to reduced tumor spheroid growth under the compressive stress.⁹⁶ Following compression, there is an upregulation in the secretion of the growth differentiation factor 15 by fibroblasts, which is essential to induce pancreatic cancer cell migration.⁹⁷ Cytoskeletal rearrangement and filopodia formation are observed in the peripheral cells, leading to a leader cell phenotype, characterized by fast and directional migration.⁹⁸ Compression stress within the tumor microenvironment also impacts the intraluminal blood vessels, which reduces perfusion, promotes hypoxia, weakens immunosurveillance, decreases drug delivery efficiency, and ultimately facilitates tumor progression.⁹⁹

The adherent cancer cells are stretched to study the effect of tensile stress.^{100–102} It was reported that at the region of low tensile stress in the contact-inhibited cells, the nuclear translocation of YAP and transcriptional coactivator with PDZ-binding motif (TAZ) is impeded by the F-actin capping and severing proteins, including CapZ and Cofilin.¹⁰¹ Nevertheless, cells under mechanical stretching exhibited upregulated YAP/TAZ nuclear translocation and, in turn, increased proliferation which is regulated by the actomyosin contractility. The upregulated YAP nuclear localization and β -catenin transcriptional activity promote cell cycle re-entry and progression through the G1 to S phase respectively, thereby enhancing proliferation in quiescent epithelial cells.¹⁰⁰ β -catenin is phosphorylated in a Src-dependent manner in mammalian MDCK epithelial cells under the tensile stress while cell

cycle arrest is observed in the S/G2 stage without proceeding to further division.¹⁰²

IV. MICROFLUIDIC TOOLS TO STUDY INVASION AND INTRAVASATION

Invasion and intravasation are pivotal steps in the metastatic process. Here, cancer cells move through confined spaces, termed confined migration, and is a crucial *in vivo* migration mode.¹⁰³ Microfluidics, an invaluable engineered model, is widely used to investigate the impact of confinement on cancer cells during migration.³⁵ In this section, we will introduce the microfluidic devices designed to mimic the confined microenvironment during invasion and intravasation as well as how cells respond to the confined spaces.

The microfluidic channels, designed to mimic constrictions during invasion and intravasation, comprise parallel migration channels created by a series of PDMS molded features through which cells migrate along a chemotaxis gradient [Figs. 3(a) and 3(b)].¹⁰⁴ The channels can be functionalized with different extracellular matrix proteins such as collagens or fibronectins to enhance cell adhesion. Most of the features were designed for studying confined cell migration typically involving narrow and long rectangular channels which cancer cells must travel,^{105–107} enabling the investigation of cell behaviors in response to varying capillary constriction geometries [Fig. 4(a)].

Davidson *et al.* designed a microfluidic chip featuring x-y axis constriction widths formed by adjacent circular PDMS posts, starting with 5 μm , then 3 μm , and finally 2 μm [Fig. 4(b)]. The design of various constrictions aims to replicate *in vivo* confined microenvironment more accurately.¹⁰⁸ A z-axis pressure-driven confinement microfluidics was developed to dynamically compress cells between two parallel surfaces [Fig. 4(c)].¹⁰⁹ By decreasing the pressure within the device, the atmospheric pressure gradually pushed the PDMS toward cells and the confinement can be precisely controlled down to sub-micrometer resolution across the surface at the square centimeter scale. Using this

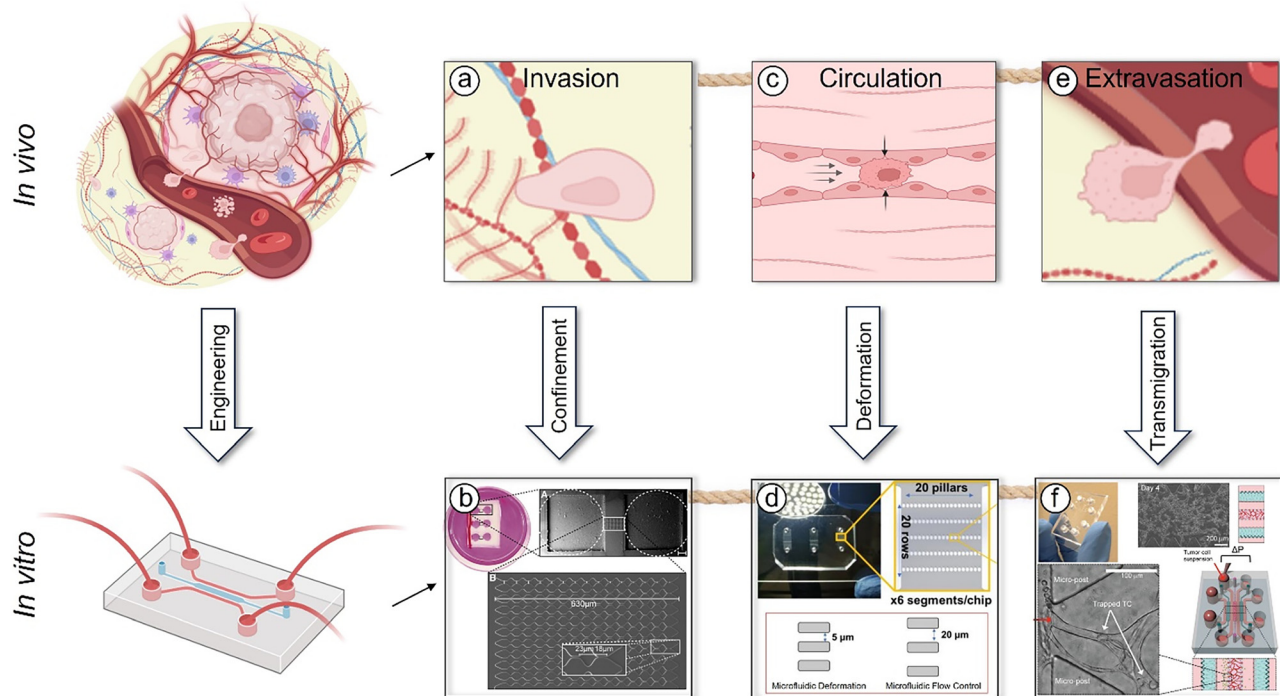


FIG. 3. From *in vivo* to *in vitro*, modeling the physical cues of metastasis in a microfluidic chip. (a) and (b) Surrounding tissue or ECM confines metastasizing cancer cells. Reproduced with permission from Lautscham *et al.*, *Biophys. J.* **109**, 900–913 (2015). Copyright 2015 Authors, licensed under a Creative Commons Attribution (CC BY) license.¹⁰⁴ (c) and (d) Constricted space in circulating system, such as small capillary, deforms CTCs. Reproduced with permission from Jiang *et al.*, *Adv. Sci.* **10**, 2201663 (2023). Copyright 2023 Authors, licensed under a Creative Commons Attribution (CC BY) 4.0 international license.¹³² (e) and (f) Arresting CTC leads to transendothelial migration (transmigration) and exiting circulatory system. Reproduced with permission from Chen *et al.*, *Nat. Protoc.* **12**, 865–880 (2017). Copyright 2017 Springer Nature Customer Service Center GmbH.¹⁶⁵

device, they manipulated the confinement degree and correlated the morphology with a study of gene expression patterns induced by the nuclear deformation and the dynamics of the nuclear lamina.

A widely used method for replicating 3D micro-topographies within *in vitro* microfluidic channels involves the use of soft lithography with PDMS, but which typically relate to less physiologically relevant stiffness (PDMS: ~800 kPa–10 MPa).¹¹⁰ Although decreasing the cross-linking level in PDMS can give rise to microfluidics with relatively low stiffness, maintaining the structural integrity of these channels presents a significant challenge.¹¹¹ The advanced method to fabricate 3D microfluidics with adjustable stiffness, along with precise control over channel dimension and morphology, remains an area of active research. Afthinos *et al.* have proposed an innovative method that employs polyacrylamide (PA) instead of the traditional PDMS-based technologies, enabling the fabrication of microfluidics with a Young's modulus of 8, 15, and 21 kPa.¹¹² This approach facilitates the production of microchannels with varying lengths, heights, and widths based on customized photolithography models, as well as ensures that the minimum microchannel confinement reached 4 μm . Nonetheless, despite these advancements, 3D PA-based microfluidics still exhibit stiffness greater than that of most physiological microenvironments encountered during cancer metastasis (as indicated in Table I). This highlights the ongoing interdisciplinary challenge within materials science and bioengineering to address this critical issue.

A. Effects of confinement on cancer cell viability

Nucleus blebs, lamin A/C enrichment and absence of lamin B, with elongated shapes were observed in cells after confined migration, followed by nuclear rupture, release of nuclear localized GFP signal, and the mislocalization of ectopic 53BP1, a DNA repair protein.^{113,114} As a consequence of the delayed accumulation of DNA repair proteins at the nuclear rupture sites, lysosomes and enzymes moved into the nucleus, leading to additional DNA damage. The upregulation of the transcription factor GATA4 resulted in the confinement-induced elongation and stabilization of mesenchymal stem cells (MSC)-like cell shape, offering crucial evidence of genotype-phenotype changes induced by migration. In addition to nuclear rupture-induced DNA damage, extensive nuclear deformation-induced DNA damage happened at replication forks during the S/G2 phase of the cell cycle due to confinement-induced replication stress, leading to increased genomic instability in metastasizing cancer cells.¹¹⁵ Endosomal sorting complexes required for transport III (ESCRT III), an enzyme involved in plasma membrane repair and post-mitotic nuclear envelope resealing, were activated and accumulated at the rupture sites to repair.¹¹⁶ Successful migrating cells through the confined microenvironment depended on the activation of DNA repair machinery located in nuclear envelope.

Microtubules, a crucial component of the cytoskeleton, maintain cell structure and play a vital role in intracellular transport.¹¹⁷ They act

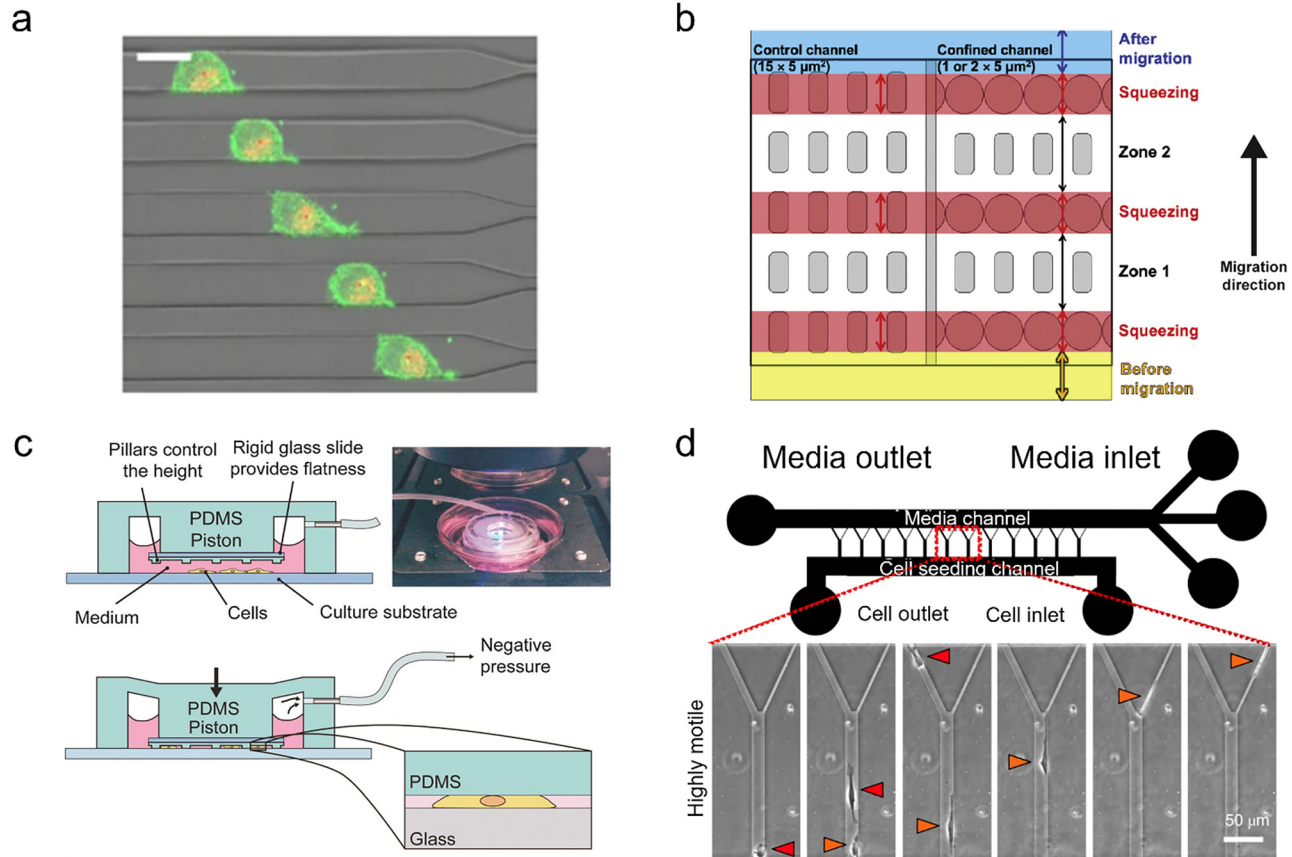


FIG. 4. Confined migration in a microfluidic platform to understand cancer invasion. (a) Representative images of cells migrating in the constriction channels. Scale bar is 20 μm. Reproduced with permission from Zhang *et al.*, *Sci. Rep.* **11**, 6529 (2021). Copyright 2021 Authors, licensed under a Creative Commons Attribution (CC BY) 4.0 international license.¹⁰⁶ (b) A simplified schematics of microfluidic device for confined cell migration. Yellow and blue are the unconfined areas for cell entrance and exit, respectively. Red is the constriction area. Zone 1 and Zone 2 indicate the unconfined areas for cells after passing through the first and second constriction, respectively. Reproduced with permission from Davidson *et al.*, *Integr. Biol.* **7**, 1534–1546 (2015). Copyright 2015 Oxford University Press.¹⁰⁸ (c) Principle of the pressure-driven cell confinement device. By decreasing the pressure, the PDMS piston is progressively pushed toward the cell (bottom diagram). Reproduced with permission from Berre *et al.*, *Integr. Biol.* **4**, 1406–1414 (2012). Copyright 2012 Oxford University Press.¹⁰⁹ (d) Schematic of the MAqCl device, with representative time-lapse micrographs of highly motile cells migrating in the MAqCl microfluidic channel. Highly motile cells are defined as cells migrating through the whole length of the feeder channel and entering either the 10-μm-wide or 3-μm-narrow branches. Reproduced with permission from Wong *et al.*, *Nat. Biomed. Eng.* **5**, 26–40 (2021). Copyright 2020 Springer Nature.¹⁰⁵

as cellular sensors assisting cancer cell movement in response to confinement and ensuring cell survival in confined microenvironment.¹¹⁸ Cytoplasmic linker-associated proteins (CLASP) are recruited, and a dedicated microtubule structure are reinforced under compression. When cells migrate through confined spaces, they align their nucleus along the migration axis. Concurrently, the CLASP at the rear of the nucleus acts to repair and reinforce the microtubule lattice, ensuring structural integrity during this process. Cells with depleted CLASP show loss of confinement induced microtubule lattice resulting in nuclear rupture and damage.

B. Effect of confinement on cancer cell migration

Successful migration requires cells to withstand large distortions in a dense microenvironment. The nucleus, as the largest and stiffest organelle within the cell body, acts as the rate-limiting factor during

the confined migration.¹¹⁹ Nuclear lamina, including A- and B-type Lamins, consists of intermediate filaments and forms interconnected networks with membrane-binding partners beneath the nuclear envelope. Lamin A/C confers cell stiffness and Lamin B1 imparts cell softness.¹²⁰ During the confined migration, cells actively optimize the expression of the Lamin A/C and Lamin B1. High Lamin A/C to Lamin B1 ratio confer stiff cells and, in turn, low migration velocity. Nevertheless, low Lamin A/C to Lamin B1 ratio leads to soft cells, fast migration but more cell death during confined migration, since soft cells are more susceptible to damage. Histone deacetylase 3 is activated by the inflow of calcium ions via stretch-activated ionic channels, leading to confinement migration-induced heterochromatin.¹²¹ The expression of heterochromatin during cell migration is strongly correlated with the degree of confinement. The chromatin accessibility decreases while part of region genes, such as chromatin silencing and DNA damage response, has been activated during this process.

When cells transverse through confinement, the nuclear envelope unfolds and stretches, resulting in the release of calcium from internal membrane stores.^{122,123} The accumulation of calcium ions in the cytoplasm lead to the phosphorylation of cytosolic phospholipase A2 (cPLA2), known as a molecular sensor for nuclear membrane tension and a crucial regulator of signaling and metabolism. The phosphorylated cPLA2 catalyzes arachidonic acid (AA), thereby potentiating the adenosine triphosphatase activity of myosin II. This process leads to enhanced contractility of the actomyosin cortex, facilitating rapid cell migration through the confinement microenvironment. A confinement-induced rapid Arp2/3-dependent perinuclear actin nucleation disrupts nuclear lamina, resulting in suppressing Lamin A/C expression and downregulation of nucleus stiffness.¹²⁴ This enables cells to rapidly and efficiently squeeze through constriction. Mitochondria actively participate in various cell migration-related activities and are observed to have a more concentrated distribution at the site of confinement among the fast-migrating subpopulation.¹⁰⁵

The “Osmotic Engine” model, reported in 2014 by the Konstantopoulos group, revealed that cancer cells, with inhibited adhesion, move with a faster velocity due to the osmotic gradient when cells are fully confined (i.e., fully blocked the microchannels).¹²⁵ Consistent with mathematical modeling, the study demonstrated that the polarized distribution of Na^+/H^+ pumps and aquaporins in the plasma membrane, in response to constriction, results in a net water and ionic influx at the cell’s leading edge and an outflow at the trailing edge, ultimately driving fast cell movement. Liu *et al.* demonstrated Focal adhesion played a dominant role in the mesenchymal-ameboid transition for slow mesenchymal cells to adapt to the confinement.¹²⁶ There is a more than sevenfold increase in migration velocity with adhesion inhibition when mesenchymal cells transit from mesenchymal migration with a velocity of $\sim 0.23 \mu\text{m}/\text{min}$ to ameboid migration ($\sim 5.3 \mu\text{m}/\text{min}$ or $\sim 1.7 \mu\text{m}/\text{min}$). Cells, with low adhesion and high cortical contractility, migrate with a velocity of approximately $5.3 \mu\text{m}/\text{min}$ while cells, with low adhesion and low cortical contractility, migrate with a velocity of around $1.7 \mu\text{m}/\text{min}$. This research established a phase diagram of migration phenotypes based on confinement, adhesion, and contractility.

Extracellular fluid viscosity is also a key mediator during cancer cell confined migration.⁴ The accumulation of the macromolecules, from the degradation of the extracellular matrix during cancer cell invasion, and the leakage of lymphatic vessels due to the compression from the primary tumor growth, increases the viscosity of the interstitial fluid.¹²⁷ The actin polymerization, in MDA-MB-231 breast cancer cells, is facilitated by the activation of the Arp 2/3, promoting the uneven distribution of Na^+/H^+ exchanger 1 (NHE1) via the actin-binding site ezrin when cells penetrate in high viscosity and confine microenvironment.⁴ This uneven distribution of NHE1 enhances cell swelling and upregulates plasma membrane tension, driving the activation of TRPV4. Consequently, the calcium influx via TRPV4 channels leads to increased RhoA-dependent cell contractility, which, in turn, leads to faster cell migration. Cancer cells that have been pre-exposed to a high-viscosity environment show an increased tendency to colonize the lungs. This behavior is linked to a TRPV4-dependent mechanical memory, which is controlled by transcriptional activities within the Hippo pathway.

C. Effect of confinement on cancer cell proliferation

Confinement can drive defects in cell division and gene expression changes, which could increase genetic instability and promote

tumorigenesis.¹²⁸ The human cervical carcinoma (HeLa) cell line observed a more than 50-fold increase in stressed cell division events under confinement than in unconfined environments, including delayed mitosis, multi-daughter cell division events, unevenly sized daughter cells, and cell death.¹²⁹ Failure in cell round-up under confinement causes unsuccessful spindle assembly, and pole splitting, leading to defects in mitotic progression.¹³⁰

V. BIOMECHANICAL FORCES SHAPE CTCs AND THEIR IMPACTS IN THE MICROCIRCULATION TRANSIT

In distant metastasis, cancer cells, either as individual cells or clusters, detach from the primary tumor and intravasate, utilizing the vascular system as a highway to traverse the body. These cells, known as CTCs, travel with the bloodstream and potentially be captured in the microcirculation—a network of small vessels and capillaries characterized by extensive branching and narrow constrictions capable of slowing CTCs.¹³¹ The residence time of CTCs in the microcirculation ranges from hours to days, during which they are exposed to various biomechanical cues, including the heterogeneity of blood shear stress and geometrical constraints [Figs. 3(c) and 3(d)].^{7,132} Nevertheless, a comprehensive understanding of these mechanical microenvironments influencing CTCs transit and their impacts on the metastatic process still remain largely unknown.

A. Cellular apoptosis under flow shear stress

While traveling in the circulatory system has been described as an expressway for distant metastasis, analysis of circulating metastasis in animal models suggested that fewer than 0.01% of CTCs successfully survive and extravasate to seed metastasis.^{133,134} *In vivo* observations, utilizing intravital two-photon imaging to track CTCs arrested in mouse lung or liver capillaries, reveal the dynamic generation of tumor microparticles,^{6,135} also known as migrasomes (size: $0.5\text{--}2 \mu\text{m}$). Long-time exposure to capillary FSS might result in the tearing of the entire cytoplasm, ultimately eliminating arrested CTCs. To understand the impact of heterogeneous FSS on cancer cells, Regmi *et al.*, developed a microfluidic device mimicking hemodynamic microenvironments [Fig. 5(b)].¹³⁶ Their works demonstrated that, more metastatic breast cancer cells perished as the increasing of culture time with FSS environments, particularly in high FSS group ($40 \text{ dyn}/\text{cm}^2$). Other studies targeting CTC clusters suggested a cluster disaggregation phenomenon.¹³⁷ Even CTCs clusters being identified as having higher metastatic potential than single CTC, they still face challenges when exposed to elevated FSS in microfluidic systems.

Given how microcirculation can regulate cancer cell apoptosis, researchers have delved into the molecular changes and dynamic responses of cell membrane and cytoskeleton, as well as the nucleus. CTCs trapped within the microvasculature, continuously exposed to FSS, alter the force balance at the cell surface and induce the activation of the membrane ion channel. The cell-surface channel protein pannexin-1 (PANX1), responding to changes in membrane tension and mechanical stresses, has been identified as a biomarker to determine malignant properties in neuroblastoma.¹³⁸ The overexpression of PANX1 in highly metastatic breast cancer cells augments ATP release, potentially aiding survival after lodging in the microvasculature.¹³⁹ Research conducted by Tan’s group suggests that cell stiffness correlates with their survival abilities [Fig. 5(a)].¹⁴⁰ Using the pharmacological reagents to re-organize cellular actomyosin structure, they found

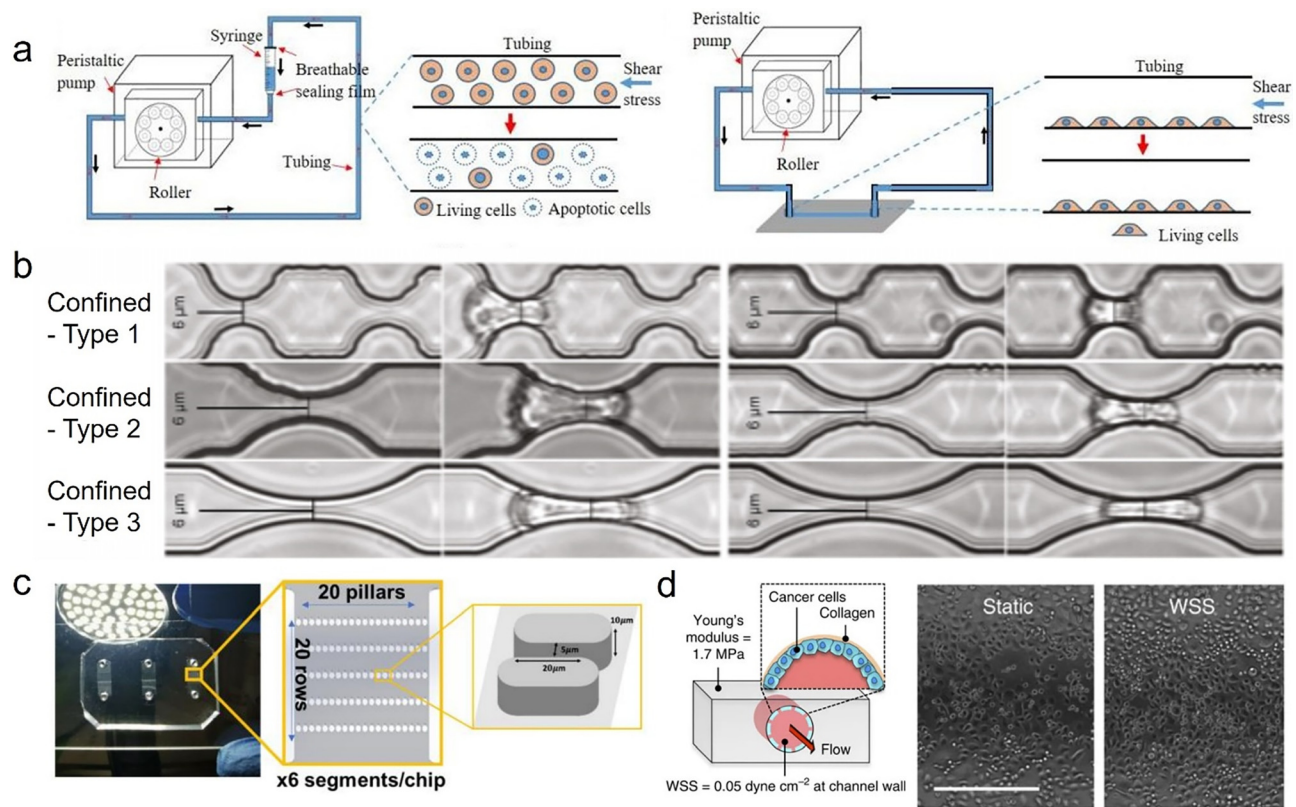


FIG. 5. Microfluidic approaches for studying cancer cells in microcirculation transit. (a) A peristaltic pump-based system to investigate the effort of fluid shear stress on cellular viability. Reproduced with permission from Xu *et al.*, *J. Cell Sci.* **135**, jcs259586 (2022). Copyright 2022 Authors, licensed under a Creative Commons Attribution (CC BY) 4.0 international license.¹⁴² (b) The use of 3D microfluidic channels drove by a constant pressure-driven flow in studying the morphological and molecular alterations of deformed cancer cells. Reproduced with permission from Cognart *et al.*, *Sci. Rep.* **10**, 6386 (2020). Copyright 2020 Authors, licensed under a Creative Commons Attribution (CC BY) 4.0 international license.¹⁵⁰ (c) Confined spaces of capillary vessel cause deformation of CTC. Mechanical deformation selects those mechanoresilient cancer cells with enhanced proliferation and chemoresistance. Reproduced with permission from Jiang *et al.*, *Adv. Sci.* **10**, 2201663 (2023). Copyright 2023 Authors, licensed under a Creative Commons Attribution (CC BY) 4.0 international license.¹³² (d) Cell motility in a lymphatic flow mimicking system using a programmable syringe pump. Reproduced with permission from Lee *et al.*, *Nat. Commun.* **8**, 14122 (2017). Copyright 2017 Authors, licensed under a Creative Commons Attribution (CC BY) 4.0 international license.¹⁵⁴

that soft tumor cells have survival advantage in resisting hemodynamic shear stress. Recent research indicated that tumor cells may adapt FSS environment and resist FSS-induced cell death via activating the RhoA-ROCK pathway and contracting actomyosin networks, leading to an upregulating of cell contractility.¹⁴¹ In addition, an *in vitro* analysis of the nucleus dynamic found a rise in nuclear size in a high FSS environment (20 dyn/cm^2) compared to low FSS environment (2 dyn/cm^2) as well as static environment (0 dyn/cm^2).¹⁴² Suspended tumor cells trigger the histone-acetylation-mediated nuclear expansion, potentially causing this shear-induced apoptosis in cancer cells. High FSS environment triggers the histone-acetylation-mediated nuclear expansion in suspended tumor cells, which potentially responds to this shear-induced apoptosis.¹⁴² Resistance of FSS is also related to the expression level of Lamin A/C, crucial for maintaining the structural integrity of the cell nucleus and providing mechanical support.¹⁴³ Comparatively, nonmalignant epithelial cells with low Lamin A/C levels perform relatively poor resistance under the FSS microenvironment. Upon knockdown of Lamin A/C, the viability of breast cancer

cells dramatically decreased only in the flow environment, but not in the static environment.

B. Navigation in microcirculation

As CTCs traverse through capillary constrictions, where the diameter is almost two to four times smaller than that of the CTCs, it has been reported in animal models that mechanical squeezing deforms not only the cytoplasm but also the cell nucleus.^{37,135} Analysis of the histologic section via using immunohistochemistry is the most traditional method to obtain the geometrical structure of capillary vessels,¹⁴⁴ whose diameters are about $3\text{--}13 \mu\text{m}$. The development of imaging systems allows for the *in situ* observation of 3D capillary bed morphologies in diverse tissues and organs.¹³⁵ In response to capillary-induced constriction, cancer cells dynamically change their migration strategies, ensuring the successful transit through capillary beds and potentially facilitating extravasation. This navigation includes two stages: (1) flowing with blood flow in a suspended state (passive

migration), and (2) squeezing into capillary vessel in an adhesive state (active migration).

Traveling in a suspended state is the most common phenotype for CTCs in circulation, wherein CTCs flow with the bloodstream and passively traverse through different organs, including the brain, liver, and lung according to cancer type. Inevitably, some CTCs circulate into capillaries in distant organs, where their diameters are smaller than the size of CTCs. Extensive *in vivo* studies using intravital imaging have revealed a shaped deformation in cancer cells while transiting capillaries.^{145,146} Notably, the confined stress between invasion and in circulation is different. The process of migration for cancer cells through the confined spaces of tissues or ECM is comparatively slow, allowing cells adequate time to adjust to the deformation.¹⁴⁵ In contrast, when cancer cells enter circulation, they are propelled rapidly by blood flow. This rapid transit requires CTCs to compress quickly in order to navigate through the narrow confines of blood vessels, potentially subjecting them to effects that are not yet fully understood.^{147–149} To further understand how these narrow constrictions impact molecular changes in breast cancer cells, Cognart *et al.* developed several types of microfluidic systems with different geometry and hydrodynamics [Fig. 5(b)].¹⁵⁰ In this microcirculation-mimicking model, the mechanical squeezing significantly increases the DNA damage in epithelial-like SK-BR-3 cells, while some epithelial-to-mesenchymal transition markers such as Snail1, Twist2, and ZEB1 were up-regulated.¹⁵⁰ Additionally, applying a mechanical selection of breast cancer cells by using a microfluidics device to mimic the mechanical deformation during capillary navigation [Fig. 5(c)].¹³² Researchers identified a unique property that the survival breast cancer cells exhibit resilience to mechanical squeezing-induced cell death. This survival subpopulation, named mechanoresilient cells, achieve enhanced proliferation and chemoresistance compared to wide-type breast cancer cells, potentially explaining how microenvironmental physical stress can promote the malignancy of metastasizing cancer cells. Particularly targeting the squeezing of CTC clusters in *in vitro* and *in vivo* small capillary vessels, cluster groups rapidly reorganized into single chain-like geometries that substantially reduce the hydrodynamic resistance exerted on cell clusters in microfluidics.¹⁵¹ In a way, the deformability of tumor cells is vital for transit in capillary vessels.^{147,152,153}

While traveling through capillary constrictions with slower flow velocities, size of CTCs is typically larger than the diameter of capillaries, which increases the possibility of CTCs trapping in capillary vessels. Subsequently, arrested CTCs transform from a suspension state to an adhesive state and move along the capillary wall, as observed in both *in vivo* and *in vitro* studies.^{7,146} When CTCs become lodged in capillaries, they can sense and convert the mechanical signals to biochemical signals, thereby activating some of the mechanotransductive pathways and adjusting their motility strategies in responding to this confined space within shear flow. In a study by Lee *et al.*, a higher level of the translocation of YAP1/TAZ to the nucleus when prostate cells were exposed to a lymphatic vasculature-mimicking FSS (~ 0.05 dyn/cm²) in a microfluidics system [Fig. 5(d)].¹⁵⁴ The activation of the ROCK-LIMK-YAP1 signal promotes migratory capacity in human prostate cancer cells, potentially promoting cancer metastasis in the lymphatic duct. Moreover, Piezo ion channels are mechanosensitive ion channels, responding to various mechanical cues such as tension, compression, and FSS. Piezo1 has been indicated as a blood flow regulation that mediates the sense of change in blood flow and assists in

maintaining vascular integrity. FSS induce the activation of Piezo 1, resulting in the calcium influx and the remodeling of the cytoskeleton.^{155,156} In cancer metastasis, Piezo channels, together with myosin II, promoted the motility of malignant cells in confined space and specifically facilitated efficient migration through microfluidic narrow channels.^{157,158} Under confined migration in capillary-like microfluidics, A-type lamins have been shown to play an essential role. Several studies indicated that downregulation of lamins A/C with a more elastic nucleus can enhance cellular motility through confined space, which facilitates the occurrence of lung metastasis.^{159–161} However, as we discussed before, low lamins A/C do not favor the resistance of FSS.¹⁴³ Further investigation is still required to understand the mechanisms by which metastasizing cancer cells regulate their lamins A/C during metastasis in microcirculation.

VI. MICROFLUIDICS TO COMPREHEND CANCER EXTRAVASATION

At the end of the circulation, CTCs must exit the bloodstream in order to establish new metastatic colonies. While the current development in imaging systems provides direct evidence of cancer cell extravasation in mouse models,^{145,162,163} the lack of a comprehensive understanding of the molecular mechanisms regulating cancer extravasation has hindered the successful targeting of this process by current anti-metastasis strategies.¹⁶⁴ The advancement of microfluidics provides a way for visualizing the process of *in vitro* extravasation and illuminating the underlying mechanisms [Figs. 3(e) and 3(f)].¹⁶⁵ Researcher has created the engineered 3D microvascular networks in microfluidic platforms (Fig. 6).^{94,165–171} Chen *et al.* reported the first microfluidic chip containing self-assembled microvascular networks in 2009,¹⁷² and this platform has been improved to apply the visualization of cancer extravasation by Chen *et al.* later [Fig. 6(b)].¹⁷⁰ In their models, once human umbilical vein endothelial cells (HUVECs) and human lung fibroblasts (HLFBs) were injected into HUVEC gel microfluidic channel, cell assembly grow with a microvascular network structure. They demonstrated that the extravasation capabilities on breast cancer cells associated with endothelial barrier function and inflammatory cytokine stimulation. The process starts with slender protrusions from tumor cells extending across the endothelium, leading to the extrusion of the rest of the cell body through the creation of small openings (about 1 μ m) in the endothelial barrier. These openings then expand to a larger size (approximately 8 μ m) to facilitate the passage of the nucleus.¹⁷⁰ Subsequently, a new on-chip human microvasculature microfluidic assay allows a visualization and dynamical quantitation of cancer extravasation over 72 h via confocal microscopy with high-resolution [Fig. 6(d)].¹⁶⁵ Certain resident cells in blood, such as platelets and neutrophils, can facilitate the efficiency of extravasation in breast (MDA-MB-231) and melanoma cells (A375-MA2).

During the process of extravasation, CTCs typically start with attachment to endothelium and finish with trans-endothelial migration to escape the circulating system. The development of 3D microvascular microfluidics is promising in enabling understanding of cancer cell extravasation, including attachment and transmigration, as well as its underlying mechanisms. Neuronal cadherin (N-cadherin), expressed by both cancer cells and endothelial cells, serves as one of the receptors that facilitates the initial arresting of cancer cells under blood flow.¹⁷³ Once CTCs attach to endothelial layer, cancer cells quick reorganize their N-cadherin distribution to promote the cell–cell junction. Subsequently, the formation of integrins-based adhesion

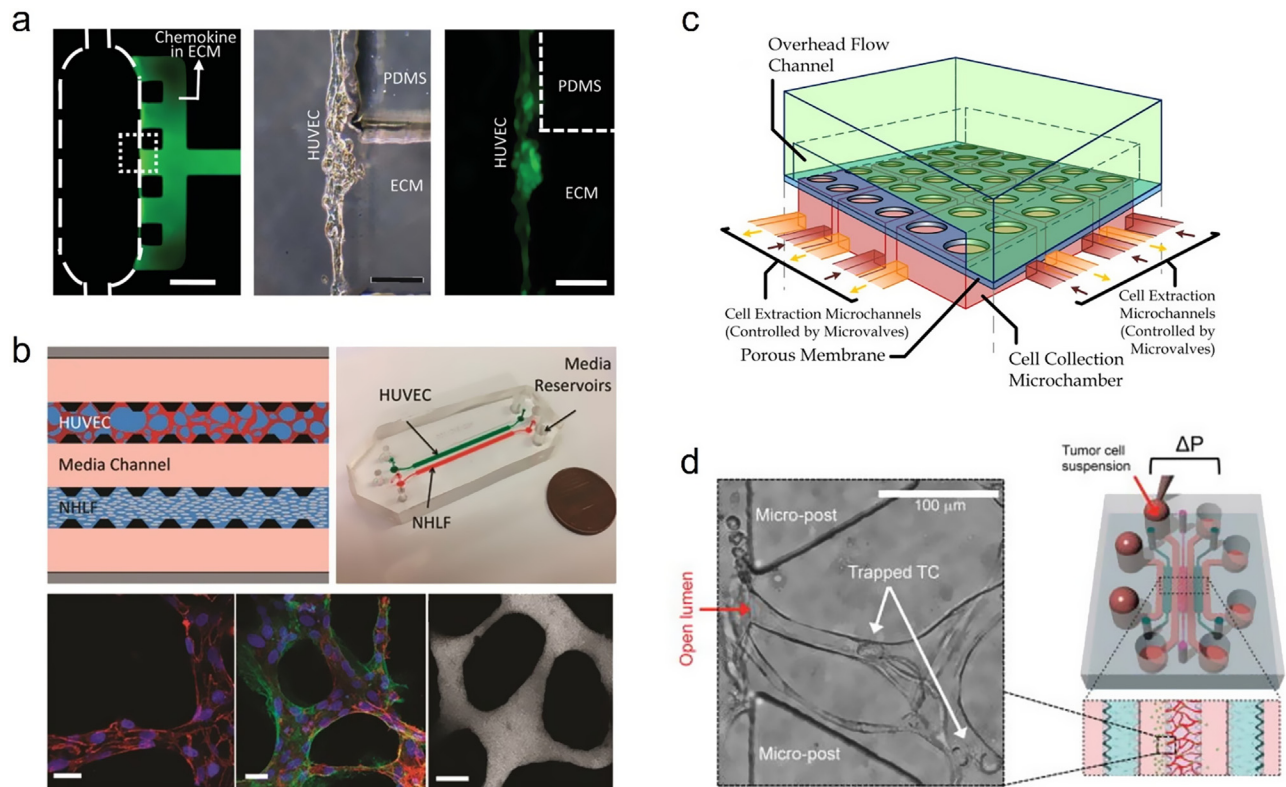


FIG. 6. Modeling extravasation on a microfluidic system. (a) A microfluidic model that includes vessel cavity, endothelium, and perivascular matrix, to understand transendothelial invasion of tumor aggregates. Reproduced with permission from Zhang *et al.*, *Lab Chip* **12**, 2837–2842 (2012). Copyright 2012 Royal Society of Chemistry Press.¹⁷¹ (b) A physiologically relevant microfluidic platform capable of accurately modeling the entire extravasation process. Reproduced with permission from Chen *et al.*, *Integr. Biol.* **5**, 1262–1271 (2013). Copyright 2013 Oxford University Press.¹⁷⁰ (c) A microfluidic model that allows the collection of extravasated cells for post-analysis. Reproduced with permission from Cui *et al.*, *Biomicrofluidics* **11**, 014105 (2017). Copyright 2017 Authors, licensed under a Creative Commons Attribution (CC BY) license.²⁰⁴ (d) A 3D microvessel bed in a microfluidics chip to understand cancer extravasation. Reproduced with permission from Chen *et al.*, *Nat. Protoc.* **12**, 865–880 (2017). Copyright 2017 Springer Nature Customer Service Center GmbH.¹⁶⁵

ensures a stable attachment, which facilitate to subsequently transmigrate.¹⁷⁴ A study on a 3D microfluidic device suggests MDA-MB-231 cells formed a integrin $\beta 1$ junction with endothelial cells once they arrest in endothelial layer, and loss of this cell–cell junction would restrain the efficiency of subsequent trans-migration.¹⁷⁵ After the formation of stable attachment, cancer cells tend to pass through the vascular endothelium by forming actin-based dynamic protrusive structures known as invadopodia.^{2,176} As an unique characteristic of cancer cells, certain pericellular proteases such as MMP9 have an enrichment of invadopodia sites which facilitate the degradation of ECM, thereby promoting transmigration and invasion.¹⁷⁷ Nevertheless, degradation is not the only way to elevate the transmigration efficiency. Since the junction gap in endothelial layer is typically smaller than cell nuclei, one study that visualized the dynamics of tumor cell nuclei suggested that tumor cells can adjust their nuclear mechanical properties during transmigration.¹⁶⁶ To facilitate this transmigration process, tumor cells reduce the stiffness of this most rigid organelle.

Here, we discussed various models designed to replicate the mechanical conditions within the microcirculation system and outlined potential mechanotransduction pathways that enable cells to

respond to these mechanical cues. Gaining insights into the behavior of CTCs within the microcirculation, understanding their ability to sense and adapt to these mechanical environments, and potentially develop a more invasive phenotype as well as their underlying mechanisms will enhance our understanding of cancer metastasis. This is particularly crucial as the microcirculation serves as the primary site where CTCs typically interact with the endothelial layer, initiating the process of extravasation. Subsequent section will describe *in vivo* and *in vitro* studies that specifically focus on metastatic colonies.

VII. MECHANICAL FEATURES ON METASTATIC NICHE

Out of the entire pool of cancer cells migrating through circulation, the vast majority face an inevitable fate of cell death. Only a minute subset, approximately 0.01%, successfully survive and establish secondary tumors in mouse experiments.¹⁷⁸ These surviving cells follow either one of the two routes: dormancy or proliferation. Typically, disseminated tumor cells (DTCs) upon entering the secondary site undergo a period of dormancy.¹⁷⁹ The dormancy or awakening of DTCs is influenced by multiple intracellular and extracellular signals. The well-known seed-and-soil theory of cancer metastasis emphasizes that specific types of tumors exhibit preferences for specific distant

metastatic niches.¹⁸⁰ While the dissemination process may seem random, successful colonization is favored by specific biomechanical properties that facilitate tumor growth in metastatic niches. Furthermore, DTCs may maintain dormancy and even possibly facing apoptosis.

Similar to the growth in primary lesions, matrix stiffness serves as a crucial environmental signal that dictates the fate of cancer cells—whether they undergo proliferation or dormancy. In both *in vivo* and *in vitro* experiments, cells tend to favor an environment with a relatively higher stiffness.²⁶ While cells seed in a relatively stiff matrix, it can prompt the nucleus translocation of YAP, facilitating the expression of Akt to resist apoptosis.¹⁸¹ Surprisingly, several studies employing AFM have verified that most metastatic colonization tissues exhibit higher stiffness as compared to healthy tissues.^{13,16,26,27,79} Microfluidic devices have been designed to mimic the physical environments of metastatic niches with the aim of understanding the biological interactions between niches and DTCs.^{182–184} A series of CXC chemokines, such as CXCL5 and CXCR2, have been identified for their contributions to breast-to-bone metastasis. Although metastatic niche with higher stiffness is beneficial to cancer cell survival and proliferation, metastasizing to soft organs, such as brain, liver, and lung with soft tissue is common in clinical medicine. Studies from Sheetz's group identified the co-function of myosin IIA, tropomyosin 2.1 and 3.1 as rigidity sensors, determining the rigidity-dependent growth.¹⁸⁵ Depletion of these rigidity sensor proteins restore tumor growth in transformed breast cancer cells, which potentially explains why DTCs adapt to a soft colonization environment.

Growth in a metastatic niche requires a nutrient supply, typically facilitated by the circulatory system. Accompany by nutrient transport, heterogeneous circulating flow exerts FSS on cancer cells in secondary colonies, relating to cell survival, proliferation, and migration. Indeed, Tan's group indicated that exposure to high FSS (~ 20 dyn/cm²) results in nucleus expansion and leads to over 60% of cell death within 12 h.¹⁴² However, a lower FSS value, reduced by 10 times or even more, facilitates chemical resistance in cancer cells.^{186,187} Except for the contribution of chemical resistance, low FSS also induces the activation of cell proliferation in metastatic breast cancer cells via enhancing the phosphorylation level and nucleus translocation of ERK.¹⁸⁸ For prostate cancer cells cultured in microfluidics with low FSS (~ 0.05 dyn/cm²), FSS elevates the expression level of TAZ and promotes its nuclear localization.¹⁸⁹ As a result, TAZ activation drives increased DNA synthesis, which promotes cell proliferation in prostate cancer cells. Furthermore, while no direct evidence currently indicates the influence of FSS on cancer migration after seeding in secondary lesions, the presence of low FSS in the interstitial flow has verified its positive contributions to early cancer dissemination.^{90,186}

Considering the heterogeneous metastatic lesions, these metastatic lesions are not always covered with tumor-favorite physical features. Certain key mutations facilitate the adaptation of cancer cells to unfavorable physical microenvironments, allowing for continued growth.¹⁹⁰ Currently, microfluidics is not the primary *in vitro* model for studying the metastatic niche. Nevertheless, its significant adaptability, particularly in addressing physical characteristics, should be highlighted. We hope the advancements in microfluidic technology will demonstrate how physical parameters in metastatic lesions, including morphological structures, extracellular viscosity, and matrix elasticity, can influence metastatic outcomes.

VIII. CONCLUDING REMARKS AND FUTURE DIRECTION

As our understanding of cancer metastasis expands, it is increasingly vital to incorporate the mechanical attributes of physiological microenvironments into our studies. Successful metastasis requires cancer cells to go through a heterogeneity of tissue or organ microenvironments and overcome the biophysical stresses exerted by these microenvironments.^{2,191,192} These stresses can drive changes in cellular morphogenesis, proliferation, migration, and even survival, which all closely bound up the development of metastases. Even cancer cells can memory these past mechanical stresses and future influence their responses in a new metastatic niche.¹¹ Our partial inability to understand these mechanics-induced cellular responses and their underlying mechanisms is due to the lack of models that accurately replicate physical microenvironments. The first conventional *in vitro* system to study metastasis was the 2D wound-healing assay, which creates a “wound” gap in a cell monolayer for observation of “healing” speeds of cells but fails to replicate the complex pathophysiological environment, particularly those physical factors.¹⁹³ Advances in microfluidic models allow the establishment of diversely physical environments with physiological relevance which will be vital to answer more complex questions during cancer metastasis.

Here, we reviewed how *in vitro* devices provide an innovative approach to modeling these physical microenvironments during cancer metastasis. We particularly highlighted microfluidic devices because of their versatility that allows for the recapitulation of physiological features (Fig. 1). These have enabled us to reveal specific and previously unknown cellular responses to mechanical microenvironments. For example, microfluidic devices mimicking the confined space during invasion suggested dynamic cancer cell migration strategies.¹⁰⁷ Tumor cells can utilize their nucleus to sense the surrounding confined space and reorganize their myosin-mediated contractility, resulting in cell polarization which highly determines their migration.^{122,194} Furthermore, squeezing through confined channels increases the likelihood of nuclear envelope rupture, driving the activation of the ESCRT III-based repair mechanism for limiting DNA damage and cell death.¹¹⁶ Even, a microfluidic platform, called microfluidic assay for quantification of cell invasion (MAqCI), has applied to evaluate the tumor aggressiveness in patient-derived primary glioblastoma specimens [Fig. 4(d)].¹⁹⁵ We can anticipate the significant role of this microfluidic technology in cancer research and further development of cancer therapy.

Understanding the role of environmental confinement is not the sole function of microfluidics, as numerous mechanobiological questions, particularly those related to the physical cues in cancer metastasis, can be addressed using these “lab-on-a-chip” systems. For example, viscoelasticity is a vital physical cue, influencing tumor growth and subsequent metastasis.^{23,196} At present, PDMS and other linearly elastic polyacrylamide are the most commonly used materials for microfluidic fabrication. However, many tissues and ECMs do not possess linearly elastic properties. Instead, they demonstrate viscoelasticity, exhibiting both viscous and elastic characteristics during deformation. Various hydrogel or collagen gel-based matrix systems reveal how matrix viscoelasticity and viscoplasticity can impact cell spreading,¹⁹⁷ migration¹⁹⁸ and, differentiation.¹⁹⁹ Similarly, other physical traits or cues such as liquid viscosity, osmotic pressure, and even cell deformation when CTCs travel into constricted circulating system can also be reconstituted in microfluidics assays. Future efforts should

focus on developing diverse and physiological microenvironments through advances in biomaterials and the fabrication of microfluidic devices.

The final goal of studying metastasis is to discover more effective strategies to combat cancer. One of the major challenges in cancer chemotherapy is the issue of drug resistance. Currently, a variety of genes, such as MUC1 and certain members of the ABC transporter gene families, have been identified for their roles in promoting chemoresistance.^{200–202} The gene expression profiles in cancer cells are highly dynamic and often affected by the physical characteristics of surrounding environments. For example, one study has shown that a hydrostatic pressure microenvironment (30 mm Hg) within a microfluidic platform can enhance the doxorubicin resistance in breast cancer cells by almost 2.5 times.²⁰³ Importantly, this increase in drug resistance is attributed to changes in gene expression rather than mutations in specific chemoresistance-related genes, meaning this change is only affected by physical cues. Tumor environment always includes diverse and complex physical cues, yet our understanding of how these physical cues influence the effect of conventional chemotherapy drugs remains limited. Nevertheless, these features that respond to mechanical stress in metastasizing cancer cells might provide new direction for anti-metastatic treatments. The evolving field of microfluidics holds promise for providing more insights in integrating mechanobiological concepts into clinical cancer therapy, potentially leading to more targeted and effective treatment strategies.

ACKNOWLEDGMENTS

This work was supported by the Institute for Health Innovation and Technology (iHealthtech) (No. A-0001415-06-00), and Mechanobiology Institute (No. A-0003467-20-00) at the National University of Singapore. We appreciate the support from the NUS Startup Grant (No. A-8001301-00-00) provided to MechanoBioEngineering Laboratory at the Department of Biomedical Engineering.

AUTHOR DECLARATIONS

Conflict of Interest

The authors have no conflicts to disclose.

Ethics Approval

Ethics approval is not required.

Author Contributions

Lanfeng Liang: Writing – original draft (equal); Writing – review & editing (equal). **Xiao Song:** Writing – original draft (equal); Writing – review & editing (equal). **Hao Zhao:** Writing – original draft (supporting); Writing – review & editing (supporting). **Chwee Teck Lim:** Supervision (lead); Writing – original draft (equal); Writing – review & editing (equal).

DATA AVAILABILITY

Data sharing is not applicable to this article as no new data were created or analyzed in this study.

REFERENCES

- H. Sung *et al.*, “Global cancer statistics 2020: GLOBOCAN estimates of incidence and mortality worldwide for 36 cancers in 185 countries,” *CA-Cancer J. Clin.* **71**, 209–249 (2021).
- C. L. Chaffer and R. A. Weinberg, “A perspective on cancer cell metastasis,” *Science* **331**, 1559–1564 (2011).
- P. S. Steeg, “Targeting metastasis,” *Nat. Rev. Cancer* **16**, 201–218 (2016).
- K. Bera *et al.*, “Extracellular fluid viscosity enhances cell migration and cancer dissemination,” *Nature* **611**, 365 (2022).
- C. D. Paul, P. Mistriotis, and K. Konstantopoulos, “Cancer cell motility: Lessons from migration in confined spaces,” *Nat. Rev. Cancer* **17**, 131 (2017).
- M. B. Headley *et al.*, “Visualization of immediate immune responses to pioneer metastatic cells in the lung,” *Nature* **531**, 513–517 (2016).
- A. Varotsos Vrynas, J. Perea Paizal, C. Bakal, and S. H. Au, “Arresting metastasis within the microcirculation,” *Clin. Exp. Metastasis* **38**, 337–342 (2021).
- D. Hanahan, “Hallmarks of cancer: New dimensions,” *Cancer Discovery* **12**, 31–46 (2022).
- K. Jiang, L. Liang, and C. T. Lim, “Engineering confining microenvironment for studying cancer metastasis,” *iScience* **24**, 102098 (2021).
- F. Martino, A. R. Perestrelo, V. Vinarský, S. Pagliari, and G. Forte, “Cellular mechanotransduction: From tension to function,” *Front. Physiol.* **9**, 824 (2018).
- E. Cambria *et al.*, “Linking cell mechanical memory and cancer metastasis,” *Nat. Rev. Cancer* **24**, 216–228 (2024).
- A. K. Scott *et al.*, “Mechanical memory stored through epigenetic remodeling reduces cell therapeutic potential,” *Biophys. J.* **122**, 1428–1444 (2023).
- I. Acerbi *et al.*, “Human breast cancer invasion and aggression correlates with ECM stiffening and immune cell infiltration,” *Integr. Biol.* **7**, 1120–1134 (2015).
- J. J. Northey *et al.*, “Stiff stroma increases breast cancer risk by inducing the oncogene ZNF217,” *J. Clin. Invest.* **130**, 5721–5737 (2020).
- A. J. Rice *et al.*, “Matrix stiffness induces epithelial-mesenchymal transition and promotes chemoresistance in pancreatic cancer cells,” *Oncogenesis* **6**, e352 (2017).
- L. Liu *et al.*, “Mechanoresponsive stem cells to target cancer metastases through biophysical cues,” *Sci. Transl. Med.* **9**, eaan2966 (2017).
- W. Ling *et al.*, “Effects of vascularity and differentiation of hepatocellular carcinoma on tumor and liver stiffness: *In vivo* and *in vitro* studies,” *Ultrasound Med. Biol.* **40**, 739–746 (2014).
- J. I. Lopez, I. Kang, W. K. You, D. M. McDonald, and V. M. Weaver, “*In situ* force mapping of mammary gland transformation,” *Integr. Biol.* **3**, 910–921 (2011).
- R. Christensen, *Theory of Viscoelasticity: An Introduction* (Elsevier, 2012).
- R. G. Wells, “The role of matrix stiffness in regulating cell behavior,” *Hepatology* **47**, 1394–1400 (2008).
- Y. M. Efremov, T. Okajima, and A. Raman, “Measuring viscoelasticity of soft biological samples using atomic force microscopy,” *Soft Matter* **16**, 64–81 (2020).
- N. Schierbaum, J. Rheinlaender, and T. E. Schäffer, “Viscoelastic properties of normal and cancerous human breast cells are affected differently by contact to adjacent cells,” *Acta Biomater.* **55**, 239–248 (2017).
- L. M. Rebelo, J. S. de Sousa, J. Mendes Filho, and M. Radmacher, “Comparison of the viscoelastic properties of cells from different kidney cancer phenotypes measured with atomic force microscopy,” *Nanotechnology* **24**, 055102 (2013).
- G. Zhang, M. Long, Z.-Z. Wu, and W.-Q. Yu, “Mechanical properties of hepatocellular carcinoma cells,” *World J. Gastroenterol.* **8**, 243 (2002).
- R. K. Jain, J. D. Martin, and T. Stylianopoulos, “The role of mechanical forces in tumor growth and therapy,” *Annu. Rev. Biomed. Eng.* **16**, 321–346 (2014).
- M. Kalli and T. Stylianopoulos, “Defining the role of solid stress and matrix stiffness in cancer cell proliferation and metastasis,” *Front. Oncol.* **8**, 55 (2018).
- H. T. Nia *et al.*, “Solid stress and elastic energy as measures of tumour mechanopathology,” *Nat. Biomed. Eng.* **1**, 0004 (2016).
- S. P. Timosenko and J. N. Goodier, *Theory of Elasticity* (McGraw-Hill, 1951).
- A. Vella, E. M. Eko, and A. del Río Hernández, “The emergence of solid stress as a potent biomechanical marker of tumour progression,” *Emerging Top. Life Sci.* **2**, 739–749 (2018).

- ³⁰E. S. Bell and J. Lammerding, "Causes and consequences of nuclear envelope alterations in tumour progression," *Eur. J. Cell Biol.* **95**, 449–464 (2016).
- ³¹C. Voutouri, C. Polydorou, P. Papageorgis, V. Gkretsi, and T. Stylianopoulos, "Hyaluronan-derived swelling of solid tumors, the contribution of collagen and cancer cells, and implications for cancer therapy," *Neoplasia* **18**, 732–741 (2016).
- ³²C. Voutouri and T. Stylianopoulos, "Accumulation of mechanical forces in tumors is related to hyaluronan content and tissue stiffness," *PLoS One* **13**, e0193801 (2018).
- ³³D. T. Butcher, T. Alliston, and V. M. Weaver, "A tense situation: Forcing tumour progression," *Nat. Rev. Cancer* **9**, 108–122 (2009).
- ³⁴C. Voutouri, F. Mpekris, P. Papageorgis, A. D. Odysseos, and T. Stylianopoulos, "Role of constitutive behavior and tumor-host mechanical interactions in the state of stress and growth of solid tumors," *PLoS One* **9**, e104717 (2014).
- ³⁵C. D. Paul, W.-C. Hung, D. Wirtz, and K. Konstantopoulos, "Engineered models of confined cell migration," *Annu. Rev. Biomed. Eng.* **18**, 159–180 (2016).
- ³⁶L. M. Coussens, B. Fingleton, and L. M. Matrisian, "Matrix metalloproteinase inhibitors and cancer: Trials and tribulations," *Science* **295**, 2387–2392 (2002).
- ³⁷J. Perea Paizal, S. H. Au, and C. Bakal, "Squeezing through the microcirculation: Survival adaptations of circulating tumour cells to seed metastasis," *Br. J. Cancer* **124**, 58–65 (2021).
- ³⁸Y. Kienast *et al.*, "Real-time imaging reveals the single steps of brain metastasis formation," *Nat. Med.* **16**, 116–122 (2010).
- ³⁹J. Swift *et al.*, "Nuclear lamin-A scales with tissue stiffness and enhances matrix-directed differentiation," *Science* **341**, 1240104 (2013).
- ⁴⁰K. P. Ivanov, M. M. Kalinina, and Y. I. Levkovich, "Blood flow velocity in capillaries of brain and muscles and its physiological significance," *Microvasc. Res.* **22**, 143–155 (1981).
- ⁴¹P. J. MacPhee, E. E. Schmidt, and A. C. Groom, "Intermittence of blood flow in liver sinusoids, studied by high-resolution in vivo microscopy," *Am. J. Physiol.* **269**, G692–G698 (1995).
- ⁴²P. R. Hoskins, "A review of the measurement of blood velocity and related quantities using Doppler ultrasound," *Proc. Inst. Mech. Eng., Part H* **213**, 391–400 (1999).
- ⁴³F. Wang *et al.*, "Flexible Doppler ultrasound device for the monitoring of blood flow velocity," *Sci. Adv.* **7**, eabi9283 (2021).
- ⁴⁴M. A. Swartz and A. W. Lund, "Lymphatic and interstitial flow in the tumour microenvironment: Linking mechanobiology with immunity," *Nat. Rev. Cancer* **12**, 210–219 (2012).
- ⁴⁵K. Kurma and C. Alix-Panabières, "Mechanobiology and survival strategies of circulating tumor cells: A process towards the invasive and metastatic phenotype," *Front. Cell Dev. Biol.* **11**, 1188499 (2023).
- ⁴⁶M. Wagner and H. Wiig, "Tumor interstitial fluid formation, characterization, and clinical implications," *Front. Oncol.* **5**, 115 (2015).
- ⁴⁷M. Pittman *et al.*, "Membrane ruffling is a mechanosensor of extracellular fluid viscosity," *Biophys. J.* **121**, 267a (2022).
- ⁴⁸C. Cao, Z. Xu, Y. Liu, B. Cheng, and F. Xu, "Enhancement effects of extracellular fluid viscosity and matrix stiffness on cancer cell mechanosensing," *Acta Mech. Sin.* **39**, 223238 (2023).
- ⁴⁹D. W. Kufe, "Mucins in cancer: Function, prognosis and therapy," *Nat. Rev. Cancer* **9**, 874–885 (2009).
- ⁵⁰R. J. Ellis, "Macromolecular crowding: Obvious but underappreciated," *Trends Biochem. Sci.* **26**, 597–604 (2001).
- ⁵¹Y. Abidine, V. M. Laurent, R. Michel, A. Duperray, and C. Verdier, "Local mechanical properties of bladder cancer cells measured by AFM as a signature of metastatic potential," *Eur. Phys. J. Plus* **130**, 202 (2015).
- ⁵²M. Lekka *et al.*, "Characterization of N-cadherin unbinding properties in non-malignant (HCV29) and malignant (T24) bladder cells," *J. Mol. Recognit.* **24**, 833–842 (2011).
- ⁵³K. Gnanachandran, S. Kędracka-Krok, J. Pabijan, and M. Lekka, "Discriminating bladder cancer cells through rheological mechanomarkers at cell and spheroid levels," *J. Biomech.* **144**, 111346 (2022).
- ⁵⁴L. Martinez-Vidal *et al.*, "Micro-mechanical fingerprints of the rat bladder change in actinic cystitis and tumor presence," *Commun. Biol.* **6**, 217 (2023).
- ⁵⁵G. Seano *et al.*, "Solid stress in brain tumours causes neuronal loss and neurological dysfunction and can be reversed by lithium," *Nat. Biomed. Eng.* **3**, 230–245 (2019).
- ⁵⁶M. M. Urbanski, M. B. Brendel, and C. V. Melendez-Vasquez, "Acute and chronic demyelinated CNS lesions exhibit opposite elastic properties," *Sci. Rep.* **9**, 999 (2019).
- ⁵⁷D. Chauvet *et al.*, "In vivo measurement of brain tumor elasticity using intraoperative shear wave elastography," *Ultraschall Med.* **37**, 584–590 (2016).
- ⁵⁸E. A. Corbin, F. Kong, C. T. Lim, W. P. King, and R. Bashir, "Biophysical properties of human breast cancer cells measured using silicon MEMS resonators and atomic force microscopy," *Lab Chip* **15**, 839–847 (2015).
- ⁵⁹S. E. Cross, Y.-S. Jin, J. Rao, and J. K. Gimzewski, in *Nano-Enabled Medical Applications* (Jenny Stanford Publishing, 2020), pp. 547–566.
- ⁶⁰S. E. Cross, Y.-S. Jin, Q.-Y. Lu, J. Rao, and J. K. Gimzewski, "Green tea extract selectively targets nanomechanics of live metastatic cancer cells," *Nanotechnology* **22**, 215101 (2011).
- ⁶¹G. Coceano *et al.*, "Investigation into local cell mechanics by atomic force microscopy mapping and optical tweezer vertical indentation," *Nanotechnology* **27**, 065102 (2015).
- ⁶²H. W. Hou *et al.*, "Deformability study of breast cancer cells using microfluidics," *Biomed. Microdevices* **11**, 557–564 (2009).
- ⁶³H.-H. Lin *et al.*, "Mechanical phenotype of cancer cells: Cell softening and loss of stiffness sensing," *Oncotarget* **6**, 20946 (2015).
- ⁶⁴M. Lekka *et al.*, "Cancer cell detection in tissue sections using AFM," *Arch. Biochem. Biophys.* **518**, 151–156 (2012).
- ⁶⁵J. Zhang, M. Nikolic, K. Tanner, and G. Scarcelli, "Rapid biomechanical imaging at low irradiation level via dual line-scanning Brillouin microscopy," *Nat. Methods* **20**, 677–681 (2023).
- ⁶⁶K. Hayashi and M. Iwata, "Stiffness of cancer cells measured with an AFM indentation method," *J. Mech. Behavior Biomed. Mater.* **49**, 105–111 (2015).
- ⁶⁷X. Zhao, Y. Zhong, T. Ye, D. Wang, and B. Mao, "Discrimination between cervical cancer cells and normal cervical cells based on longitudinal elasticity using atomic force microscopy," *Nanoscale Res. Lett.* **10**, 482 (2015).
- ⁶⁸S. Iyer, R. M. Gaikwad, V. Subba-Rao, C. D. Woodworth, and I. Sokolov, "Atomic force microscopy detects differences in the surface brush of normal and cancerous cells," *Nat. Nanotechnol.* **4**, 389–393 (2009).
- ⁶⁹E. Lopez-Crapez *et al.*, "Mechanical signatures of human colon cancers," *Sci. Rep.* **12**, 12475 (2022).
- ⁷⁰Y. Yang *et al.*, in *IEEE International Ultrasonics Symposium (IUS)* (IEEE, 2018).
- ⁷¹E. L. Opie and M. B. Rothbard, "Osmotic homeostasis maintained by mammalian liver, kidney, and other tissues," *J. Exp. Med.* **97**, 483–497 (1953).
- ⁷²M. Tian *et al.*, "The nanomechanical signature of liver cancer tissues and its molecular origin," *Nanoscale* **7**, 12998–13010 (2015).
- ⁷³H. S. Brown *et al.*, "Measurement of normal portal venous blood flow by Doppler ultrasound," *Gut* **30**, 503–509 (1989).
- ⁷⁴E. Giannopoulou *et al.*, "The inhibition of aromatase alters the mechanical and rheological properties of non-small-cell lung cancer cell lines affecting cell migration," *Biochim. Biophys. Acta* **1853**, 328–337 (2015).
- ⁷⁵J. Gostek *et al.*, "Nano-characterization of two closely related melanoma cell lines with different metastatic potential," *Eur. Biophys. J.* **44**, 49–55 (2015).
- ⁷⁶B. Erdogan *et al.*, "Cancer-associated fibroblasts promote directional cancer cell migration by aligning fibronectin," *J. Cell Biol.* **216**, 3799–3816 (2017).
- ⁷⁷M. Prabhune, G. Belge, A. Dotzauer, J. Bullerdiek, and M. Radmacher, "Comparison of mechanical properties of normal and malignant thyroid cells," *Micron* **43**, 1267–1272 (2012).
- ⁷⁸A. Levillain *et al.*, "Mechanical properties of breast, kidney, and thyroid tumours measured by AFM: Relationship with tissue structure," *Materialia* **25**, 101555 (2022).
- ⁷⁹Y. Shen, T. Schmidt, and A. Diz-Muñoz, "Protocol on tissue preparation and measurement of tumor stiffness in primary and metastatic colorectal cancer samples with an atomic force microscope," *STAR Protoc.* **1**, 100167 (2020).
- ⁸⁰X. Cao *et al.*, "A tumor-on-a-chip system with bioprinted blood and lymphatic vessel pair," *Adv. Funct. Mater.* **29**, 1807173 (2019).
- ⁸¹A. Spencer *et al.*, "A high-throughput mechanofluidic screening platform for investigating tumor cell adhesion during metastasis," *Lab on a Chip* **16**, 142–152 (2016).

- ⁸²K. G. Birmingham *et al.*, “Lymph node subcapsular sinus microenvironment-on-a-chip modeling shear flow relevant to lymphatic metastasis and immune cell homing,” *iScience* **23**, 101751 (2020).
- ⁸³K. M. Lugo-Cintrón *et al.*, “Breast fibroblasts and ECM components modulate breast cancer cell migration through the secretion of MMPs in a 3D microfluidic co-culture model,” *Cancers* **12**, 1173 (2020).
- ⁸⁴X. Li and J. Wang, “Mechanical tumor microenvironment and transduction: Cytoskeleton mediates cancer cell invasion and metastasis,” *Int. J. Biol. Sci.* **16**, 2014–2028 (2020).
- ⁸⁵S. Dupont *et al.*, “Role of YAP/TAZ in mechanotransduction,” *Nature* **474**, 179–183 (2011).
- ⁸⁶H. W. Park *et al.*, “Alternative Wnt signaling activates YAP/TAZ,” *Cell* **162**, 780–794 (2015).
- ⁸⁷A. Elosegui-Artola *et al.*, “Force triggers YAP nuclear entry by regulating transport across nuclear pores,” *Cell* **171**, 1397–1410 (2017).
- ⁸⁸J. M. Lamar *et al.*, “The Hippo pathway target, YAP, promotes metastasis through its TEAD-interaction domain,” *Proc. Natl. Acad. Sci. U. S. A.* **109**, E2441–E2450 (2012).
- ⁸⁹W. H. Lee *et al.*, “TRPV4 plays a role in breast cancer cell migration via Ca²⁺-dependent activation of AKT and downregulation of E-cadherin cell cortex protein,” *Oncogenesis* **6**, e338 (2017).
- ⁹⁰W. J. Polacheck, J. L. Charest, and R. D. Kamm, “Interstitial flow influences direction of tumor cell migration through competing mechanisms,” *Proc. Natl. Acad. Sci. U. S. A.* **108**, 11115–11120 (2011).
- ⁹¹H. Y. Choi *et al.*, “Hydrodynamic shear stress promotes epithelial-mesenchymal transition by downregulating ERK and GSK3 β activities,” *Breast Cancer Res.* **21**, 6 (2019).
- ⁹²S. Liu *et al.*, “Fluid shear stress induces epithelial-mesenchymal transition (EMT) in Hep-2 cells,” *Oncotarget* **7**, 32876 (2016).
- ⁹³A. Nyga, U. Cheema, and M. Loizidou, “3D tumour models: novel in vitro approaches to cancer studies,” *J. Cell Commun. Signal.* **5**(3), 239–248 (2011).
- ⁹⁴S. M. Bhat *et al.*, “3D tumor angiogenesis models: Recent advances and challenges,” *J. Cancer Res. Clin. Oncol.* **147**, 3477–3494 (2021).
- ⁹⁵G. Cheng, J. Tse, R. K. Jain, and L. L. Munn, “Micro-environmental mechanical stress controls tumor spheroid size and morphology by suppressing proliferation and inducing apoptosis in cancer cells,” *PLoS One* **4**, e4632 (2009).
- ⁹⁶M. Delarue *et al.*, “Compressive stress inhibits proliferation in tumor spheroids through a volume limitation,” *Biophys. J.* **107**, 1821–1828 (2014).
- ⁹⁷M. Kalli, P. Papageorgis, V. Gkretsi, and T. Stylianopoulos, “Solid stress facilitates fibroblasts activation to promote pancreatic cancer cell migration,” *Ann. Biomed. Eng.* **46**, 657–669 (2018).
- ⁹⁸J. M. Tse *et al.*, “Mechanical compression drives cancer cells toward invasive phenotype,” *Proc. Natl. Acad. Sci. U. S. A.* **109**, 911–916 (2012).
- ⁹⁹F. Mpekris, S. Angeli, A. P. Pirentis, and T. Stylianopoulos, “Stress-mediated progression of solid tumors: Effect of mechanical stress on tissue oxygenation, cancer cell proliferation, and drug delivery,” *Biomech. Model. Mechanobiol.* **14**, 1391–1402 (2015).
- ¹⁰⁰B. W. Benham-Pyle, B. L. Pruitt, and W. J. Nelson, “Mechanical strain induces E-cadherin-dependent Yap1 and β -catenin activation to drive cell cycle entry,” *Science* **348**, 1024–1027 (2015).
- ¹⁰¹G. C. Fletcher *et al.*, “Mechanical strain regulates the Hippo pathway in *Drosophila*,” *Development* **145**, dev159467 (2018).
- ¹⁰²B. W. Benham-Pyle, J. Y. Sim, K. C. Hart, B. L. Pruitt, and W. J. Nelson, “Increasing β -catenin/Wnt3A activity levels drive mechanical strain-induced cell cycle progression through mitosis,” *eLife* **5**, e19799 (2016).
- ¹⁰³P. K. Chaudhuri, B. C. Low, and C. T. Lim, “Mechanobiology of tumor growth,” *Chem. Rev.* **118**, 6499–6515 (2018).
- ¹⁰⁴L. A. Lautscham *et al.*, “Migration in confined 3D environments is determined by a combination of adhesiveness, nuclear volume, contractility, and cell stiffness,” *Biophys. J.* **109**, 900–913 (2015).
- ¹⁰⁵X. Zhang and M. Mak, “Biophysical informatics approach for quantifying phenotypic heterogeneity in cancer cell migration in confined microenvironments,” *Bioinformatics* **37**, 2042–2052 (2021).
- ¹⁰⁶X. Zhang, T. Chan, and M. Mak, “Morphodynamic signatures of MDA-MB-231 single cells and cell doublets undergoing invasion in confined microenvironments,” *Sci. Rep.* **11**, 6529 (2021).
- ¹⁰⁷A. W. Holle *et al.*, “Cancer cells invade confined microchannels via a self-directed mesenchymal-to-amoeboid transition,” *Nano Lett.* **19**, 2280–2290 (2019).
- ¹⁰⁸P. M. Davidson, J. Sliz, P. Isermann, C. Denais, and J. Lammerding, “Design of a microfluidic device to quantify dynamic intra-nuclear deformation during cell migration through confining environments,” *Integr. Biol.* **7**, 1534–1546 (2015).
- ¹⁰⁹M. Le Berre, J. Aubertin, and M. Piel, “Fine control of nuclear confinement identifies a threshold deformation leading to lamina rupture and induction of specific genes,” *Integr. Biol.* **4**, 1406–1414 (2012).
- ¹¹⁰R. Seghir and S. Arscott, “Extended PDMS stiffness range for flexible systems,” *Sens. Actuators, A* **230**, 33–39 (2015).
- ¹¹¹H. Yoshie *et al.*, “Traction force screening enabled by compliant PDMS elastomers,” *Biophys. J.* **114**, 2194–2199 (2018).
- ¹¹²A. Afthinos *et al.*, “Migration and 3D traction force measurements inside compliant microchannels,” *Nano Lett.* **22**, 7318–7327 (2022).
- ¹¹³J. Irianto *et al.*, “DNA damage follows repair factor depletion and portends genome variation in cancer cells after pore migration,” *Curr. Biol.* **27**, 210–223 (2017).
- ¹¹⁴P. Shah, K. Wolf, and J. Lammerding, “Bursting the bubble—nuclear envelope rupture as a path to genomic instability?,” *Trends Cell Biol.* **27**, 546–555 (2017).
- ¹¹⁵P. Shah *et al.*, “Nuclear deformation causes DNA damage by increasing replication stress,” *Curr. Biol.* **31**, 753–765. e756 (2021).
- ¹¹⁶M. Raab *et al.*, “ESCRT III repairs nuclear envelope ruptures during cell migration to limit DNA damage and cell death,” *Science* **352**, 359–362 (2016).
- ¹¹⁷R. D. Vale, “The molecular motor toolbox for intracellular transport,” *Cell* **112**, 467–480 (2003).
- ¹¹⁸R. J. Ju *et al.*, “Compression-dependent microtubule reinforcement comprises a mechanostat which enables cells to navigate confined environments,” *bioRxiv* (2022).
- ¹¹⁹Y. Kalukula, A. D. Stephens, J. Lammerding, and S. Gabriele, “Mechanics and functional consequences of nuclear deformations,” *Nat. Rev. Mol. Cell Biol.* **23**, 583–602 (2022).
- ¹²⁰T. Harada *et al.*, “Nuclear lamin stiffness is a barrier to 3D migration, but softness can limit survival,” *J. Cell Biol.* **204**, 669–682 (2014).
- ¹²¹C.-R. Hsia *et al.*, “Confined migration induces heterochromatin formation and alters chromatin accessibility,” *iScience* **25**, 104978 (2022).
- ¹²²A. J. Lomakin *et al.*, “The nucleus acts as a ruler tailoring cell responses to spatial constraints,” *Science* **370**, eaba2894 (2020).
- ¹²³C. L. Yankaskas *et al.*, “The fluid shear stress sensor TRPM7 regulates tumor cell intravasation,” *Sci. Adv.* **7**, eabh3457 (2021).
- ¹²⁴H.-R. Thiam *et al.*, “Perinuclear Arp2/3-driven actin polymerization enables nuclear deformation to facilitate cell migration through complex environments,” *Nat. Commun.* **7**, 10997 (2016).
- ¹²⁵K. M. Stroka *et al.*, “Water permeation drives tumor cell migration in confined microenvironments,” *Cell* **157**, 611–623 (2014).
- ¹²⁶Y.-J. Liu *et al.*, “Confinement and low adhesion induce fast amoeboid migration of slow mesenchymal cells,” *Cell* **160**, 659–672 (2015).
- ¹²⁷J. Yin, X. Kong, and W. Lin, “Noninvasive cancer diagnosis *in vivo* based on a viscosity-activated near-infrared fluorescent probe,” *Anal. Chem.* **93**, 2072–2081 (2021).
- ¹²⁸C. R. Pfeifer *et al.*, “Constricted migration increases DNA damage and independently represses cell cycle,” *Mol. Biol. Cell* **29**, 1948–1962 (2018).
- ¹²⁹H. T. K. Tse, W. M. Weaver, and D. Di Carlo, “Increased asymmetric and multi-daughter cell division in mechanically confined microenvironments,” *PLoS One* **7**, e38986 (2012).
- ¹³⁰O. M. Lancaster *et al.*, “Mitotic rounding alters cell geometry to ensure efficient bipolar spindle formation,” *Dev. Cell* **25**, 270–283 (2013).
- ¹³¹P. Paterlini-Brechot and N. L. Benali, “Circulating tumor cells (CTC) detection: Clinical impact and future directions,” *Cancer Lett.* **253**, 180–204 (2007).
- ¹³²K. Jiang *et al.*, “Deleterious mechanical deformation selects mechanoresilient cancer cells with enhanced proliferation and chemoresistance,” *Adv. Sci.* **10**, 2201663 (2023).

- ¹³³K. Yoshida, T. Fujikawa, A. Tanabe, and K. Sakurai, "Quantitative analysis of distribution and fate of human lung cancer emboli labeled with ¹²⁵I-5-iodo-2'-deoxyuridine in nude mice," *Surg. Today* **23**, 979–983 (1993).
- ¹³⁴L. Weiss, U. Nannmark, B. R. Johansson, and U. Bagge, "Lethal deformation of cancer cells in the microcirculation: A potential rate regulator of hematogenous metastasis," *Int. J. Cancer* **50**, 103–107 (1992).
- ¹³⁵J. Wu *et al.*, "Iterative tomography with digital adaptive optics permits hour-long intravital observation of 3D subcellular dynamics at millisecond scale," *Cell* **184**, 3318–3332 (2021).
- ¹³⁶S. Regmi, A. Fu, and K. Q. Luo, "High shear stresses under exercise condition destroy circulating tumor cells in a microfluidic system," *Sci. Rep.* **7**, 39975 (2017).
- ¹³⁷A. Marrella *et al.*, "High blood flow shear stress values are associated with circulating tumor cells cluster disaggregation in a multi-channel microfluidic device," *PLoS One* **16**, e0245536 (2021).
- ¹³⁸S. Langlois *et al.*, "Inhibition of PAXX1 channels reduces the malignant properties of human high-risk neuroblastoma," *J. Cancer* **14**, 689 (2023).
- ¹³⁹P. W. Furlow *et al.*, "Mechanosensitive pannexin-1 channels mediate microvascular metastatic cell survival," *Nat. Cell Biol.* **17**, 943–952 (2015).
- ¹⁴⁰Y. Xin *et al.*, "Mechanics and actomyosin-dependent survival/chemoresistance of suspended tumor cells in shear flow," *Biophys. J.* **116**, 1803–1814 (2019).
- ¹⁴¹D. L. Moose *et al.*, "Cancer cells resist mechanical destruction in circulation via RhoA/actomyosin-dependent mechano-adaptation," *Cell Rep.* **30**, 3864–3874 (2020).
- ¹⁴²Z. Xu *et al.*, "Fluid shear stress regulates the survival of circulating tumor cells via nuclear expansion," *J. Cell Sci.* **135**, jcs259586 (2022).
- ¹⁴³M. J. Mitchell *et al.*, "Lamin A/C deficiency reduces circulating tumor cell resistance to fluid shear stress," *Am. J. Physiol.* **309**, C736–C746 (2015).
- ¹⁴⁴C. Zhou, E. S. Crockett, L. Batten, I. F. McMurtry, and T. Stevens, "Pulmonary vascular dysfunction secondary to pulmonary arterial hypertension: Insights gained through retrograde perfusion," *Am. J. Physiol.* **314**, L835–L845 (2018).
- ¹⁴⁵J. Condeelis and J. E. Segall, "Intravital imaging of cell movement in tumours," *Nat. Rev. Cancer* **3**, 921–930 (2003).
- ¹⁴⁶D. Entenberg, M. H. Oktay, and J. S. Condeelis, "Intravital imaging to study cancer progression and metastasis," *Nat. Rev. Cancer* **23**, 25–42 (2023).
- ¹⁴⁷T.-H. Kim *et al.*, "Cancer cells become less deformable and more invasive with activation of β -adrenergic signaling," *J. Cell Sci.* **129**, 4563–4575 (2016).
- ¹⁴⁸E. M. Balzer *et al.*, "Physical confinement alters tumor cell adhesion and migration phenotypes," *FASEB J.* **26**, 4045–4056 (2012).
- ¹⁴⁹K. Jiang *et al.*, "Deleterious mechanical deformation selects mechanoresilient cancer cells with enhanced proliferation and chemoresistance," *bioRxiv* (2022).
- ¹⁵⁰H. A. Cognart, J.-L. Viovy, and C. Villard, "Fluid shear stress coupled with narrow constrictions induce cell type-dependent morphological and molecular changes in SK-BR-3 and MDA-MB-231 cells," *Sci. Rep.* **10**, 6386 (2020).
- ¹⁵¹S. H. Au *et al.*, "Clusters of circulating tumor cells traverse capillary-sized vessels," *Proc. Natl. Acad. Sci. U. S. A.* **113**, 4947–4952 (2016).
- ¹⁵²J. H. Jeong, Y. Sugii, M. Minamiyama, and K. Okamoto, "Measurement of RBC deformation and velocity in capillaries in vivo," *Microvasc. Res.* **71**, 212–217 (2006).
- ¹⁵³S. Byun *et al.*, "Characterizing deformability and surface friction of cancer cells," *Proc. Natl. Acad. Sci. U. S. A.* **110**, 7580–7585 (2013).
- ¹⁵⁴H. J. Lee *et al.*, "Fluid shear stress activates YAP1 to promote cancer cell motility," *Nat. Commun.* **8**, 14122 (2017).
- ¹⁵⁵D. J. Beech, "Endothelial Piezo1 channels as sensors of exercise," *J. Physiol.* **596**, 979–984 (2018).
- ¹⁵⁶M. Young, A. H. Lewis, and J. Grandl, "Physics of mechanotransduction by Piezo ion channels," *J. Gen. Physiol.* **154**, e202113044 (2022).
- ¹⁵⁷W.-C. Hung *et al.*, "Confinement sensing and signal optimization via Piezo1/PKA and Myosin II pathways," *Cell Rep.* **15**, 1430–1441 (2016).
- ¹⁵⁸C. Pardo-Pastor *et al.*, "Piezo2 channel regulates RhoA and actin cytoskeleton to promote cell mechanobiological responses," *Proc. Natl. Acad. Sci. U. S. A.* **115**, 1925–1930 (2018).
- ¹⁵⁹E. S. Bell *et al.*, "Low lamin A levels enhance confined cell migration and metastatic capacity in breast cancer," *Oncogene* **41**, 4211–4230 (2022).
- ¹⁶⁰Y. Wang, J. Jiang, L. He, G. Gong, and X. Wu, "Effect of lamin-A expression on migration and nuclear stability of ovarian cancer cells," *Gynecol. Oncol.* **152**, 166–176 (2019).
- ¹⁶¹F. Roncato *et al.*, "Reduced lamin A/C does not facilitate cancer cell transendothelial migration but compromises lung metastasis," *Cancers* **13**, 2383 (2021).
- ¹⁶²C. Pan *et al.*, "Deep learning reveals cancer metastasis and therapeutic antibody targeting in the entire body," *Cell* **179**, 1661–1676 (2019).
- ¹⁶³D. Entenberg *et al.*, "A permanent window for the murine lung enables high-resolution imaging of cancer metastasis," *Nat. Methods* **15**, 73–80 (2018).
- ¹⁶⁴Y.-H. V. Ma, K. Middleton, L. You, and Y. Sun, "A review of microfluidic approaches for investigating cancer extravasation during metastasis," *Microsyst. Nanoeng.* **4**, 17104 (2018).
- ¹⁶⁵M. B. Chen *et al.*, "On-chip human microvasculature assay for visualization and quantification of tumor cell extravasation dynamics," *Nat. Protoc.* **12**, 865–880 (2017).
- ¹⁶⁶A. B. Roberts *et al.*, "Tumor cell nuclei soften during transendothelial migration," *J. Biomech.* **121**, 110400 (2021).
- ¹⁶⁷S. Kim, H. Lee, M. Chung, and N. L. Jeon, "Engineering of functional, perfusable 3D microvascular networks on a chip," *Lab Chip* **13**, 1489–1500 (2013).
- ¹⁶⁸X. Cheng and K. Cheng, "Visualizing cancer extravasation: From mechanistic studies to drug development," *Cancer Metastasis Rev.* **40**, 71–88 (2021).
- ¹⁶⁹Y. Shin *et al.*, "Microfluidic assay for simultaneous culture of multiple cell types on surfaces or within hydrogels," *Nat. Protoc.* **7**, 1247–1259 (2012).
- ¹⁷⁰M. B. Chen, J. A. Whisler, J. S. Jeon, and R. D. Kamm, "Mechanisms of tumor cell extravasation in an *in vitro* microvascular network platform," *Integr. Biol.* **5**, 1262–1271 (2013).
- ¹⁷¹Q. Zhang, T. Liu, and J. Qin, "A microfluidic-based device for study of transendothelial invasion of tumor aggregates in realtime," *Lab Chip* **12**, 2837–2842 (2012).
- ¹⁷²X. Chen *et al.*, "Prevascularization of a fibrin-based tissue construct accelerates the formation of functional anastomosis with host vasculature," *Tissue Eng., Part A* **15**, 1363–1371 (2009).
- ¹⁷³G. Li, K. Satyamoorthy, and M. Herlyn, "N-cadherin-mediated intercellular interactions promote survival and migration of melanoma cells," *Cancer Res.* **61**, 3819–3825 (2001).
- ¹⁷⁴C. Strell and F. Entschladen, "Extravasation of leukocytes in comparison to tumor cells," *Cell Commun. Signaling* **6**, 10 (2008).
- ¹⁷⁵M. B. Chen, J. M. Lamar, R. Li, R. O. Hynes, and R. D. Kamm, "Elucidation of the roles of tumor integrin β 1 in the extravasation stage of the metastasis cascade," *Cancer Res.* **76**, 2513–2524 (2016).
- ¹⁷⁶H. Paz, N. Pathak, and J. Yang, "Invading one step at a time: The role of invadopodia in tumor metastasis," *Oncogene* **33**, 4193–4202 (2014).
- ¹⁷⁷A. M. Weaver, "Invadopodia: Specialized cell structures for cancer invasion," *Clin. Exp. Metastasis* **23**, 97–105 (2006).
- ¹⁷⁸I. J. Fidler and M. L. Kripke, "Metastasis results from preexisting variant cells within a malignant tumor," *Science* **197**, 893–895 (1977).
- ¹⁷⁹A. Dasgupta, A. R. Lim, and C. M. Ghajar, "Circulating and disseminated tumor cells: Harbingers or initiators of metastasis?," *Mol. Oncol.* **11**, 40–61 (2017).
- ¹⁸⁰L. C. Hofbauer *et al.*, "Novel approaches to target the microenvironment of bone metastasis," *Nat. Rev. Clin. Oncol.* **18**, 488–505 (2021).
- ¹⁸¹B. J. Thompson, "YAP/TAZ: Drivers of tumor growth, metastasis, and resistance to therapy," *Bioessays* **42**, 1900162 (2020).
- ¹⁸²S. Bersini *et al.*, "A microfluidic 3D *in vitro* model for specificity of breast cancer metastasis to bone," *Biomaterials* **35**, 2454–2461 (2014).
- ¹⁸³W. Zhu *et al.*, "Engineering a biomimetic three-dimensional nanostructured bone model for breast cancer bone metastasis study," *Acta Biomater.* **14**, 164–174 (2015).
- ¹⁸⁴F. Salamanna *et al.*, "A human 3D *in vitro* model to assess the relationship between osteoporosis and dissemination to bone of breast cancer tumor cells," *J. Cell. Physiol.* **232**, 1826–1834 (2017).
- ¹⁸⁵B. Yang *et al.*, "Stopping transformed cancer cell growth by rigidity sensing," *Nat. Mater.* **19**, 239–250 (2020).
- ¹⁸⁶Q. Huang *et al.*, "Fluid shear stress and tumor metastasis," *Am. J. Cancer Res.* **8**, 763 (2018).
- ¹⁸⁷U. L. Triantafyllou, S. Park, and Y. Kim, "Fluid shear stress induces drug resistance to doxorubicin and paclitaxel in the breast cancer cell line MCF7," *Adv. Ther.* **2**, 1800112 (2019).

- ¹⁸⁸X. Qin *et al.*, “Low shear stress induces ERK nuclear localization and YAP activation to control the proliferation of breast cancer cells,” *Biochem. Biophys. Res. Commun.* **510**, 219–223 (2019).
- ¹⁸⁹H. J. Lee, A. Ewere, M. F. Diaz, and P. L. Wenzel, “TAZ responds to fluid shear stress to regulate the cell cycle,” *Cell Cycle* **17**, 147–153 (2018).
- ¹⁹⁰F. Spill, D. S. Reynolds, R. D. Kamm, and M. H. Zaman, “Impact of the physical microenvironment on tumor progression and metastasis,” *Curr. Opin. Biotechnol.* **40**, 41–48 (2016).
- ¹⁹¹B. Emon, J. Bauer, Y. Jain, B. Jung, and T. Saif, “Biophysics of tumor microenvironment and cancer metastasis—A mini review,” *Comput. Struct. Biotechnol. J.* **16**, 279–287 (2018).
- ¹⁹²V. Gensbittel *et al.*, “Mechanical adaptability of tumor cells in metastasis,” *Dev. Cell* **56**, 164 (2020).
- ¹⁹³C. Decaestecker, O. Debeir, P. Van Ham, and R. Kiss, “Can anti-migratory drugs be screened in vitro? A review of 2D and 3D assays for the quantitative analysis of cell migration,” *Med. Res. Rev.* **27**, 149–176 (2007).
- ¹⁹⁴V. Venturini *et al.*, “The nucleus measures shape changes for cellular proprioception to control dynamic cell behavior,” *Science* **370**, eaba2644 (2020).
- ¹⁹⁵B. S. Wong *et al.*, “A microfluidic cell-migration assay for the prediction of progression-free survival and recurrence time of patients with glioblastoma,” *Nat. Biomed. Eng.* **5**, 26–40 (2021).
- ¹⁹⁶O. Chaudhuri, J. Cooper-White, P. A. Janmey, D. J. Mooney, and V. B. Shenoy, “Effects of extracellular matrix viscoelasticity on cellular behaviour,” *Nature* **584**, 535–546 (2020).
- ¹⁹⁷M. Caiazzo *et al.*, “Defined three-dimensional microenvironments boost induction of pluripotency,” *Nat. Mater.* **15**, 344–352 (2016).
- ¹⁹⁸K. M. Wisdom *et al.*, “Matrix mechanical plasticity regulates cancer cell migration through confining microenvironments,” *Nat. Commun.* **9**, 4144 (2018).
- ¹⁹⁹H.-P. Lee, R. Stowers, and O. Chaudhuri, “Volume expansion and TRPV4 activation regulate stem cell fate in three-dimensional microenvironments,” *Nat. Commun.* **10**, 529 (2019).
- ²⁰⁰S. Nath *et al.*, “MUC1 induces drug resistance in pancreatic cancer cells via upregulation of multidrug resistance genes,” *Oncogenesis* **2**, e51 (2013).
- ²⁰¹M. P. Ween, M. R. Armstrong, M. K. Oehler, and C. Ricciardelli, “The role of ABC transporters in ovarian cancer progression and chemoresistance,” *Crit. Rev. Oncol./Hematol.* **96**, 220–256 (2015).
- ²⁰²R.-R. Begicevic and M. Falasca, “ABC transporters in cancer stem cells: Beyond chemoresistance,” *Int. J. Mol. Sci.* **18**, 2362 (2017).
- ²⁰³M. Shang *et al.*, “Microfluidic studies of hydrostatic pressure-enhanced doxorubicin resistance in human breast cancer cells,” *Lab Chip* **21**, 746–754 (2021).
- ²⁰⁴X. Cui *et al.*, “A microfluidic device for isolation and characterization of transendothelial migrating cancer cells,” *Biomicrofluidics* **11**, 014105 (2017).